ĽUBOR KRESÁK

THE DIRECTION DISTRIBUTION OF TELESCOPIC METEORS

CONTENTS

1. Introduction

During the last years an enhanced attention is paid to the smallest solid particles of interplanetary matter and their situation in the solar system. Accurate photographic measurements of positions and velocities, which only are liable for providing full informations on the heliocentric orbits of these bodies, are practically restricted to the particles with masses of the order of 10^{-2} to 10 grams. The masses below the lower limit correspond to faint naked-eye and telescopic meteors which form the connecting link to the invisible particles of interplanetary dust. Recent investigations indicate that the invisible micrometeoric dust occurs in such abundance that its contribution to the earth's mass considerably surpasses the contribution of bodies exhibiting visible meteor phenomena; however our insights into the orbits of these particles are rather uncertain and an analogy with the orbits of bright meteors and fireballs seems to be by no means well-founded.

The question whether, in what numbers and in which regions of meteor streams of various types the smallest meteoric particles are presents, is one of the most pressing problems of meteor astronomy. With regard to the origin and evolution of meteor streams two questions whose solution may be sought just in the range of telescopic meteors merit special attention. The first is the relation between the sizes of shower meteors and the dispersion of their orbits, which may present us with certain informations on the distribution of momentum among individual meteoroids at their separation from the parent comet (or at another process of their origin) and hence on the conditions of the stream's formation. The second is the confirmation of the systematic shift of the orbits of smaller particles due to a persistent operation of the Poynting-Robertson effect, which may give us some evidence of the time elapsed since the moment of separation, and thus even of the age of the stream. The solution of the former problem necessitates the derivation of a considerable number of accurate

radiants belonging to extremely faint shower meteors, which at the present stage of technical development is reserved for the telescopic observations, and the derivation of geocentric velocities with an accuracy superior to that obtained by the present radio-echo technique. The solution of the latter question bears upon the abundance of smaller particles within the main stream, which may be confirmed by using a properly adapted method ot telescopic or radio-echo observation. Of these two methods the telescopic observation allows to reach fainter particles and seems therefore to be more promising at present.

In the telescopic and radio-echo observations of meteor showers the background of sporadic meteors appears as a serious disturbing factor, far more difficult for eliminating than in the photographic or naked-eye work. The main task of the present study was to fix the features of this background, to design the most suitable manner for suppressing its influence on the observations of meteor showers, and to develop—as a counterpart to the method described on p. 64 — 68 of the present volume—another method for statistical researches on the shower activity in the range of telescopic meteors.

The validity of some consequences, deduced by applying the Law of Chance to rather schematical presumptions, had to be in several points reconciled with the direct observations. For this purpose the reductions of a series of telescopic observations, made in the years 1946—1953 at the Skalnaté Pleso Observatory, have been included in the present paper. As far as is known to the author, the statistics of directions derived from this series is more extensive than those published previously elsewhere. Therefore some additional problems could be treated on its base, which do not refer to the origin and evolution of meteor streams but to the geometrical and physiological conditions of visibility, valid for telescopic meteors.

Finally, some features of the telescopic meteor orbits in the solar system, following from the distribution of apparent radiants in relation to the apex and ecliptic, have been investigated.

2. *The Apparent Distribution of Directions for Meteors Penetrating Isotropically a Plane Atmospheric Layer*

First, let us consider a simplified case that meteors move isotropically with respect to the Earth, and appear in a plane layer perpendicular to the vertical of the observing place. If the telescope is directed towards the point A, having an altitude H above the horizon (Fig. 1), then the meteors whose paths projected on the sphere form with the vertical an angle greater than ϑ but smaller than $\vartheta + d\vartheta$ come from the apparent radiants situated inside the spherical triangle ABC. Under the conditions mentioned above the expected density of radiants in different parts of the triangle will be proportional to $\sin H$.

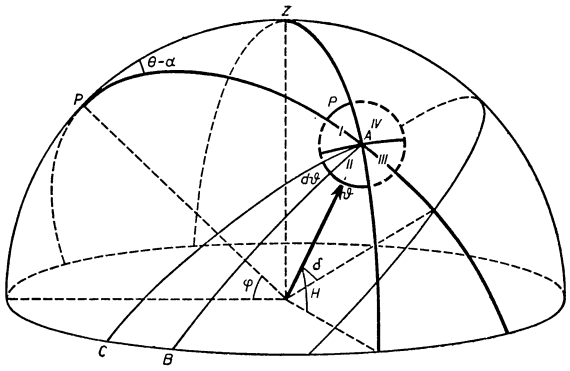

Figure 1.

To simplify the problem, let us divide the position angles of the meteor paths into four quadrants. The first quadrant (I) comprises the meteors moving from the right and above, the second (II) from the right and below, the third (III) from the left and below and the fourth (IV) from the left and above. In order to find the probability p, that the direction of a given meteor falls into a given quadrant, we have to compute the lengths of the sections of the horizontal circles falling into the respective quadrant l, multiply them with the due densities of the radiants d, integrate them between the limits of altitude $h\left(O, \frac{\pi}{2}\right)$, and divide by the integral of densities over the whole hemisphere. In this way we obtain for the second quadrant:

$$l_{II} = \cos h \cos^{-1}(\cot H \tan h)^* \text{ for } 0 < h < H \quad (1)$$

$$d_{II} = \sin h \quad (2)$$

$$p_{II} = \frac{\int_0^H \sin h \cos h \cos^{-1}(\cot H \tan h)\, dh}{\int_0^{\frac{\pi}{2}} 2\pi \sin h \cos h\, dh} =$$

$$= \frac{1}{\pi} \int_0^H \sin h \cos h \cos^{-1}(\cot H \tan h)\, dh \quad (3)$$

* The symbol $\cos^{-1}$ denotes the inverse function to cosine, somewhere used to be written as arccos.

The integral (3) is directly solvable. After a series of adaptations, including intergration per partes and two substitutions, we obtain the final result:

$$p_{II} = \frac{1}{4}(1 - \cos H) = \frac{1}{2}\sin^2\frac{H}{2} \qquad (4)$$

Similarly,

$$p_{III} = p_{II} = \frac{1}{2}\sin^2\frac{H}{2} \qquad (5)$$

$$p_I = p_{IV} = \frac{1}{2}(1 - p_{II}) = \frac{1}{2}\cos^2\frac{H}{2} \qquad (6)$$

The resulting distribution of directions, computed from the formulae (4)—(6), is tabulated below for the argument H graduated five by five degrees. The predominance of the directions from above is striking for the lower elevations, reaching 90 % at $H = 36°.9$, and 99 % at $H = 11.°5$.

Table I

$H°$	p_I p_{IV}	p_{II} p_{III}
0	0.50000	0.00000
5	0.49905	0.00095
10	0.49620	0.00380
15	0.49148	0.00852
20	0.48492	0.01508
25	0.47658	0.02342
30	0.46651	0.03349
35	0.45479	0.04521
40	0.44151	0.05849
45	0.42678	0.07322
50	0.41070	0.08930
55	0.39339	0.10661
60	0.37500	0.12500
65	0.35565	0.14435
70	0.33551	0.16449
75	0.31470	0.18530
80	0.29341	0.20659
85	0.27179	0.22821
90	0.25000	0.25000

3. The Effect of the Earth's Curvature

The computed distribution of directions, represented by the values of the Table I, slightly differs from the real one, as the condition (2) is not strictly fulfilled. Actually, the region in which the meteors become visible is not a plane but a relatively thin layer, delimited by two concentric spherical surfaces and the plane of the horizon. The visible paths of faint (telescopic) meteors are short compared with their heights; consequently, we may replace the space occupied by them, with a satisfactory approximation, by an infinitesimally thin, spherically curved layer.

Denoting by v the real height of this layer above the earth's surface, and by r the radius of the earth, we may derive a new relation for the density of sporadic radiants in the elevation h. This density is obviousky given by the projektion of the curved atmospheric layer into the plone perpendicular to the direction of penetrating meteors. Therefrom we find tha

a) for $h \leqq -\cos^{-1}\frac{r}{r+v}$:

$$d = 0 \qquad (7)$$

b) for $-\cos^{-1}\frac{r}{r+v} \leqq h \leqq +\cos^{-1}\frac{r}{r+v}$:

$$d = \frac{1}{2}\sin h + \frac{r(1-\cos h)+v}{2\sqrt{2rv+v^2}} \qquad (8)$$

c) for $+\cos^{-1}\frac{r}{r+v} \leqq h \leqq \frac{\pi}{2}$:

$$d = \sin h \qquad (9)$$

For the sake of abbreviation, let us introduce the following notation:

$$M = \frac{r+v}{2\sqrt{2rv+v^2}} \qquad (10)$$

$$N = \frac{r}{2\sqrt{2rv+v^2}} \qquad (11)$$

$$\omega = \cos^{-1}\frac{r}{r+v} = \cos^{-1}\frac{N}{M} \qquad (12)$$

Then we have for the probability p_{II} that the direction of a meteor, observed in the altitude H, will fall into the second quadrant, the following modified formulae:

a) for $0 \leqq H \leqq \omega$:

$$p_{II} = \frac{\pi\int_{-\omega}^{-H}\left(\frac{1}{2}\sin h + M - N\cos h\right)\cos h\,dh + \int_{-H}^{H}\left(\frac{1}{2}\sin h + M - N\cos h\right)\cos h\cos^{-1}(\cot H\tan h)\,dh}{2\pi\int_{-\omega}^{\omega}\left(\frac{1}{2}\sin h + M - N\cos h\right)\cos h\,dh + 2\pi\int_{\omega}^{\frac{\pi}{2}}\sin h\cos h\,dh} \qquad (13)$$

b) for $\omega \leqq H \leqq \frac{\pi}{2}$:

$$p_{II} = \frac{\int_{-\omega}^{\omega} \left(\frac{1}{2}\sin h + M - N\cos h\right)\cos h \cos^{-1}(\cot H \tan h)\,\mathrm{d}h + \int_{\omega}^{H} \sin h \cos h \cos^{-1}(\cot H \tan h)\,\mathrm{d}h}{2\pi \int_{-\omega}^{\omega} \left(\frac{1}{2}\sin h + M - N\cos h\right)\cos h\,\mathrm{d}h + 2\pi \int_{\omega}^{\frac{\pi}{2}} \sin h \cos h\,\mathrm{d}h} \tag{14}$$

The expressions (13), (14), though different, may be reduced to the same form, viz.

$$p_{II} = \frac{\frac{1}{\pi}\int_{0}^{H} \sin h \cos h \cos^{-1}(\cot H \tan h)\,\mathrm{d}h + \int_{0}^{\omega} \left(M - N\cos h - \frac{1}{2}\sin h\right)\cos h\,\mathrm{d}h}{2\int_{0}^{\frac{\pi}{2}} \sin h \cos h\,\mathrm{d}h + 4\int_{0}^{\omega} \left(M - N\cos h - \frac{1}{2}\sin h\right)\cos h\,\mathrm{d}h} \tag{15}$$

where all integrals can be found directly. After some adaptations we obtain:

$$p_{II} = \frac{1}{4}\left(1 - \frac{\cos H}{2(1 - N\omega)}\right) \tag{16}$$

or, substituing again the values of r, v from the relations (11), (12):

$$p_{II} = \frac{1}{4}\left(1 - \frac{\cos H}{2 - \frac{r}{\sqrt{2rv + v^2}}\cos^{-1}\frac{r}{r + v}}\right) \tag{17}$$

The comparison of (4) and (17) shows that the curvature of the Earth appears only in the coefficient of cosH (for a plane atmosphere equal to one, otherwise somewhat less), which is a function of the ratio of meteors' height to the Earth's radius.

Using the formula (17), we can derive the theoretical distribution of directions under different assumptions as to the real heights of telescopic meteors. These heights being known with a sufficient accuracy from double observations [1, 2], we may choose the round values 80 and 100 km as surely comprising the main part of the atmospheric layer in which telescopic meteors actually appear. For these two heights and the radius of the observing place $r = 6366.13$ km we obtain the values of M, N, and ω, which are summarized in the Table II. The resulting distribution of directions is represented in the Table III, giving the dependence of p_{II} upon v and H. The probabilities of the directions falling into the remaining three quadrants, may be readily found from the obvious relations:

$$p_{III} = p_{II} \tag{18}$$

$$p_{I} = p_{IV} = \frac{1}{2} - p_{II} \tag{19}$$

Table II

	$v = 80$ km	$v = 100$ km
M	3.18355	2.85406
N	3.14404	2.80992
ω	0.15771	0.17610
$\omega°$	9°026	10°090

Table III

$H°$	p_{II}		
	plane atmosphere	curved atmosphere	
		$v = 80$ km	$v = 100$ km
0	0.00000	0.00206	0.00256
5	0.00095	0.00300	0.00350
10	0.00380	0.00583	0.00632
15	0.00852	0.01051	0.01099
20	0.01508	0.01701	0.01749
25	0.02342	0.02529	0.02575
30	0.03349	0.03528	0.03571
35	0.04521	0.04690	0.04731
40	0.05849	0.06007	0.06045
45	0.07322	0.07468	0.07504
50	0.08930	0.09063	0.09095
55	0.10661	0.10779	0.10808
60	0.12500	0.12603	0.12628
65	0.14435	0.14522	0.14543
70	0.16449	0.16520	0.16537
75	0.18530	0.18583	0.18596
80	0.20659	0.20695	0.20703
85	0.22821	0.22839	0.22843
90	0.25000	0.25000	0.25000

4. The Effect of the Earth's Attraction

There is still another effect which alters the distribution of the sporadic radiants on the sphere against the simple $\sin h$-law, by increasing the densities of the radiants in the lower altitudes. The orbits of the meteors approaching the Earth are perturbed by the Earth's gravity, and altered in such way that they meet the atmosphere under extended angles. The alteration of the direction of the meteor's motion increases with decreasing height, geocentric velocity, and altitude of the radiant point. With a satisfactory approximation, we may consider the nearly rectilinear intercept of the meteor's orbit in the vicinity of the Earth as changed into a hyperbola with the Earth's centre as focus. The angle formed by the visible (atmospheric) section of the hyperbola and its asymptote represents the deviation of the meteor's path from the original direction which, with regard to its tendency, is called the zenith attraction.

As the basic formulae for computing the effect of zenith attraction are commonly known, it seems superfluous to repeat them in the general form. However, we shall give a transformation which is most convenient for our purpose.

Firstly, let us consider a radiant whose unperturbed altitude (i. e. the original altitude unaffected by the zenith attraction) is h. The Earth's gravity makes the radiant shifted along its vertical circle into an apparent position nearer to the zenith by an amount which we shall denote by $\Phi(h)$. Secondly, let us consider a radiant in the apparent altitude h. In order to obtain the original unperturbed altitude, we must diminish the perturbed one by an amount which we shall denote by $\psi(h)$. The corrections $\Phi(h)$ and $\psi(h)$ enabling the passage from the unperturbed to the perturbed position and inversely are given by the following expressions:

$$\Phi(h) = \frac{\pi}{4} - \frac{h}{2} - \sin^{-1}\left[\frac{u}{w}\sin\left(\frac{\pi}{4} - \frac{h}{2}\right)\right] \quad (20)$$

$$\psi(h) = 2\tan^{-1}\left[\frac{u-w}{u+w}\tan\left(\frac{\pi}{4} - \frac{h}{2}\right)\right] \quad (21)$$

Between $\Phi(h)$ and $\psi(h)$ the following relations hold true:

$$\Phi(h) = -\psi[h + \Phi(h)] \quad (22)$$

$$\psi(h) = -\Phi[h + \psi(h)] \quad (23)$$

In the formulae (20), (21) u and w denote the unperturbed and perturbed geocentric velocity of the meteor. These are correlated by the equation:

$$w^2 = u^2 + 2rg \quad (24)$$

where r denotes the distance of the meteor's visible path from the Earth's centre, and g the due constant of the Earth's gravity. Numerically, we may put

$$2rg = 125 \text{ km}^2 \text{ sec}^{-2} \quad (25)$$

The deviations $\Phi(h)$ and $\psi(h)$ for a particular meteor may be found by inserting the velocities u, w and the altitude of the radiant h into (20) and (21).

The geocentric velocity of a meteor depends on the semimajor axis of its orbit, and on the elongation of its radiant from the apex. For our investigations we have computed the effect of zenith attraction for a uniform geocentric velocity of sporadic meteors, using the mean of 10,933 McKinley's radar measurements [3], i. e.

$$w = 42.8 \text{ km sec}^{-1} \quad (26)$$

The simplification of the problem by assuming a uniform geocentric velocity introduces perhaps some errors into the final results. However, it considerably facilitates the computations, and as even the influence of zenith attraction on the apparent distribution of directions is of the second order the deviations due to the non-uniform distribution of velocities may be safely neglected. Besides, it is impossible to obtain any general solution because the distribution of velocities undergoes strong daily and yearly variations due to the changing position of the apex with respect to the horizon; and each division into subgroups according to the altitudes of the apex would reduce the statistical importance of the observations to be compared with the theory.

The values of $\Phi(h)$ and $\psi(h)$ for different altitudes h, graduated five by five degrees, are given in Table IV. It may be noted that the assumption (26), used throughout, is equivalent with the assumption of meteors moving in parabolic orbits, whose apparent radiants lie in the elongation of about 69° from the apex.

There are two possible ways how to modify the formulae for computing the a priori probabilities of various directions by allowance for the effect of zenith attraction. First of all, we can improve the expressions (2) or (7—9), giving the density of radiants in different points of the sphere, by taking into account the convergency of radiants due to the differential zenith attraction; otherwise we can replace the areas for integrating the number of radiants (1) by the areas, which would be occupied by the same radiants if the Earth's gravity would not perturb the motion of the me-

Table IV

$h°$	$\Phi(h)°$	$\Psi(h)°$
	+	—
0	1.956	2.024
5	1.797	1.855
10	1.650	1.699
15	1.511	1.553
20	1.381	1.417
25	1.259	1.290
30	1.142	1.169
35	1.031	1.054
40	0.924	0.944
45	0.822	0.839
50	0.722	0.737
55	0.626	0.638
60	0.532	0.542
65	0.441	0.449
70	0.351	0.357
75	0.262	0.267
80	0.174	0.177
85	0.087	0.088
90	0.000	0.000

teors. Out of the two methods, the latter is more suitable for our purpose.

Formula (15), including the effect of the Earth's curvature, is too complicated for further improvements. However, as both the effects of the Earth's curvature and attraction are of the second order, we may consider them separately and add, with a satisfactory approximation, the increments of p_{II} due to them to the unaffected values of Table I.

Now let us examine how the basic formula (3) will be modified by taking into account the effect zenith attraction and neglecting the effect of the Earth's curvature.

Under the assumptions given in the 2nd paragraph (isotropic distribution of geocentric meteor directions, plane atmosphere) the solution remains similar to (1)—(3) except three modifications. They are:

1. The apparent radiant altitudes h belong to the radiants whose unperturbed altitudes are $h + \psi(h)$. Hence

$$l'_{II} = \cos h \cos^{-1} (\cot [H + \psi (H)] \tan h) \quad (27)$$

2. The density of unperturbed radiants in the altitude h corresponds to the density of perturbed radiants in the altitude $h + \Phi (h)$. Hence

$$d'_{II} = \sin [h + \Phi (h)] \quad (28)$$

3. The range of integration $<0, H>$ for perturbed radiants corresponds to the range $<\psi (0), H + \psi (H)>$ for unperturbed radiants. Hence

$$p'_{II} = \frac{\int_{\psi(0)}^{H+\psi(H)} \sin [h + \Phi(h)] \cos h \cos^{-1} \cot[H + \psi(H)] \tan h) \, dh}{2\pi \int_{\psi(0)}^{\frac{\pi}{2}} \sin [h + \Phi(h)] \cos h \, dh} . \quad (29)$$

The ratio

$$x = \frac{\int_{\psi(0)}^{\frac{\pi}{2}} \sin [h + \Phi (h)] \cos h \, dh}{\int_{0}^{\frac{\pi}{2}} \sin h \cos h \, dh} = 2 \int_{\psi(0)}^{\frac{\pi}{2}} \sin [h + \Phi(h)] \cos h \, dh \quad (30)$$

gives the relative increase of the number of sporadic radiants above the horizon due to the zenith attraction. Thus we find:

$$x = 1.03546 \quad (31)$$

which means that the meteor rates are increased by about 3.5 %.

In the expression (29) the denominator is independent of H and a common numerical value can be worked out for all altitudes of the field of view. Numerical integrations in the numerator have been performed for selected round altitudes H; the values corresponding to other altitudes have been found by interpolation. The results of the computations are given in the second column of Table V. To make allowance for the Earth's curvature, the increments of p'_{II} according to (17) have been added to p'_{II} and the results have been arranged in the last two columns of the Table. It is seen that the effect of the Earth's curvature considerably exceeds the effect of the zenith attraction except for the highest altitudes.

Table V

$H°$	p'_{II}		
	plane atmosphere	curved atmosphere	
		$v = 80$ km	$v = 100$ km
0	0.00000	0.00206	0.00256
5	0.00115	0.00320	0.00370
10	0.00420	0.00623	0.00672
15	0.00910	0.01109	0.01157
20	0.01583	0.01776	0.01824
25	0.02431	0.02618	0.02664
30	0.03450	0.03629	0.03672
35	0.04630	0.04799	0.04840
40	0.05963	0.06121	0.06159
45	0.07438	0.07584	0.07620
50	0.09044	0.09177	0.09209
55	0.10770	0.10888	0.10917
60	0.12601	0.12704	0.12729
65	0.14524	0.14611	0.14632
70	0.16524	0.16595	0.16612
75	0.18588	0.18641	0.18654
80	0.20699	0.20735	0.20743
85	0.22841	0.22859	0.22863
90	0.25000	0.25000	0.25000

The values of p'_{II} for a curved atmosphere may be actually somewhat higher due to the fact that the two effects were considered separately; however, the deviations may be expected in the last decimals only. The errors coming from the unexactness of the procedure of numerical integration are about equally large; thus we may expect that the unexactnes of the data in Table V will be generally between the limits 10^{-5} to 10^{-4}.

5. The Application of a Simplified Formula

The same factors which alter the distribution of meteor directions against the formula (3) are valid also for altering the hourly rates of meteors. The simple formula for deriving the zenithal hourly rate F_z of a shower which has its radiant point in the altitude h,

$$F_z = F \operatorname{cosec} h \tag{32}$$

is frequently substituted by empirical formulae expressing with a closer approximation the actual conditions in the atmospheric layer in which meteors appear. Hoffmeister [4] gives the following improved formula:

$$F_z = 0.993\, F \operatorname{cosec} (h + 6.5°) \tag{33}$$

whereas English observers use to apply a similar formula, according to Prentice [5]:

$$F_z = F \operatorname{cosec} (h + 6°) \tag{34}$$

It seems reasonable to compare the results of the preceding two paragraphs with those which would be obtained from a formula of that kind, by assuming a new density function for the distribution of sporadic radiants,

$$D_{II} = \sin (h + k) \tag{35}$$

and retaining the other factors in the equation (3) unchanged. The value of the constant k, which fits best to the results of the preceding rigorous computations, may be found by comparison of numerical probabilities obtained in this way with those given in Table VI.

If the density of sporadic radiants in the altitude h is proportional to $\sin (h + k)$ instead of $\sin h$, the formula (3) has to be modified as follows:

$$P_{II} = \frac{\int_{-k}^{H} \sin (h + k) \cos h\, E(h,H)\, \mathrm{d}h}{2\pi \int_{-k}^{\frac{\pi}{2}} \sin (h + k) \cos h\, \mathrm{d}h} \tag{36}$$

where

$$E(h,H) = \cos^{-1} (\tan h \cot H) \quad \text{if} \quad -H < h < \frac{\pi}{2} \tag{37}$$

and

$$E(h,H) = \pi \quad \text{if} \quad -k < h < -H \tag{38}$$

The integral in the numerator of (36) cannot be found directly. Before applying numerical integrations we shall transform this expression so as to separate the members of different orders, remembering that $k \doteq 0.1$ or smaller. The most convenient transformation may be written in the form:

$$P_{II} = \frac{c_1 + c_2 + c'_2 + c_3}{c'_1 + c''_2} \tag{39}$$

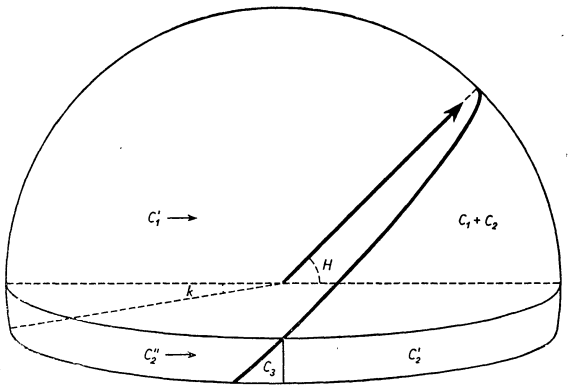

Figure 2.

The subscripts 1—3 indicate the terms of the first to third order; the geometrical interpretation of

the division is schematically represented in Figure 2. The quantities on the right side of (39) are defined by the following relations:

$$c_1 = \cos k \int_0^H \sin h \cos h \cos^{-1}(\tan h \cot H)\, \mathrm{d}h =$$

$$= \frac{\pi}{4} \cos k (1 - \cos H) = p_{\mathrm{II}} \pi \cos k \qquad (40)$$

$$c_1' = 2\pi \cos k \int_{-k}^{\frac{\pi}{2}} \sin h \cos h \, \mathrm{d}h = \pi \cos^3 k \qquad (41)$$

$$c_2 = \sin k \int_0^H \cos^2 h \cos^{-1}(\tan h \cot H)\, \mathrm{d}h =$$

$$= F(H) \sin k \qquad (42)$$

$$c_2' = \frac{\pi}{2} \int_{-k}^{0} \sin(h + k) \cos h \, \mathrm{d}h = \frac{\pi k}{4} \sin k \qquad (43)$$

$$c_2'' = 2\pi \sin k \int_{-k}^{\frac{\pi}{2}} \cos^2 h \, \mathrm{d}h =$$

$$= \frac{\pi}{2} \sin k (\pi + 2k + \sin 2k) \qquad (44)$$

$$c_3 = \int_{-k}^{0} \sin(h + k) \cos h \left[E(h,H) - \frac{\pi}{2} \right] \mathrm{d}h =$$

$$= G(k,H) \qquad (45)$$

Substituting the values (40)—(45) into (39) we obtain the final formula:

$$P_{\mathrm{II}} = \frac{p_{\mathrm{II}} + \left[\frac{1}{\pi} F(H) + \frac{k}{4} \right] \tan k + \frac{1}{\pi} G(k,H) \sec k}{1 + \left(\frac{\pi}{2} + k \right) \tan k} \qquad (46)$$

The values of the integrals $F(H)$ and $G(k, H)$ have been found by the process of numerical integration. For evaluating $F(H)$ Simpson formula was employed troughout; for evaluating $G(k, H)$ Simpson and Dufton formulae: the former for $G(k, H) > 10^{-4}$, the latter for the rest. The integrations have been performed for selected altitudes H supposing $k = 2°$, $4°$, and $6°$; for other altitudes, five by five degrees, $F(H)$ and $G(k, H)$ have been found by interpolation. The resulting values of $\frac{1}{\pi} F(H) \tan k$ and $\frac{1}{\pi} G(k,H) \sec k$ are tabulated below.

Inserting the above quantities into (46) we readily obtain the probabilities P_{II} for different k. They are arranged in Table VII.

Now the question remains, how to choose the constant k so as to bring the functions $p_{\mathrm{II}}'(H)$ and $P_{\mathrm{II}}(k, H)$ into the closest possible coincidence. It is obvious, that this value of k is given by the relation:

$$\int_0^{\frac{\pi}{2}} [p_{\mathrm{II}}'(H) - P_{\mathrm{II}}(k,H)]\, \nu(H) \cos H \, \mathrm{d}H = 0 \qquad (47)$$

where $\nu(H)$ indicates the proportional frequency of meteor paths in the altitude H. The course of the function $\nu(H)$ depends on several factors which

Table VI

$H°$	$\frac{1}{\pi} F(H) \tan k$			$\frac{1}{\pi} G(k, H) \sec k$		
	$k = 2°$	$k = 4°$	$k = 6°$	$k = 2°$	$k = 4°$	$k = 6°$
0	0.00000	0.00000	0.00000	0.00030	0.00122	0.00275
5	0.00097	0.00194	0.00292	0.00003	0.00021	0.00078
10	0.00193	0.00387	0.00582	0.00001	0.00010	0.00035
15	0.00289	0.00578	0.00869	0.00001	0.00007	0.00023
20	0.00383	0.00767	0.01152	0.00001	0.00005	0.00017
25	0.00475	0.00951	0.01429	0.00000	0.00004	0.00013
30	0.00565	0.01131	0.01700	0.00000	0.00003	0.00011
35	0.00652	0.01305	0.01962	0.00000	0.00003	0.00009
40	0.00736	0.01473	0.02214	0.00000	0.00002	0.00007
45	0.00816	0.01634	0.02457	0.00000	0.00002	0.00006
50	0.00893	0.01788	0.02688	0.00000	0.00002	0.00005
55	0.00966	0.01934	0.02907	0.00000	0.00001	0.00004
60	0.01035	0.02072	0.03115	0.00000	0.00001	0.00003
65	0.01100	0.02202	0.03310	0.00000	0.00001	0.00003
70	0.01161	0.02324	0.03494	0.00000	0.00001	0.00002
75	0.01218	0.02439	0.03666	0.00000	0.00000	0.00002
80	0.01272	0.02546	0.03827	0.00000	0.00000	0.00001
85	0.01322	0.02648	0.03980	0.00000	0.00000	0.00001
90	0.01371	0.02746	0.04127	0.00000	0.00000	0.00000

Table VII

$H°$	P_{II}			
	$k = 0°$	$k = 2°$	$k = 4°$	$k = 6°$
0	0.00000	0.00058	0.00219	0.00488
5	0.00095	0.00214	0.00388	0.00629
10	0.00380	0.00573	0.00806	0.01082
15	0.00852	0.01110	0.01399	0.01717
20	0.01508	0.01820	0.02155	0.02510
25	0.02342	0.02697	0.03067	0.03451
30	0.03349	0.03735	0.04131	0.04536
35	0.04521	0.04927	0.05339	0.05754
40	0.05849	0.06264	0.06680	0.07096
45	0.07322	0.07735	0.08146	0.08554
50	0.08930	0.09330	0.09726	0.10117
55	0.10661	0,11038	0.11409	0.11774
60	0.12500	0,12845	0.13183	0.13513
65	0.14435	0.14739	0.15035	0.15324
70	0.16449	0.16704	0.16951	0.17193
75	0.18530	0.18728	0.18920	0.19108
80	0.20659	0.20795	0.20926	0.21054
85	0.22821	0.22890	0.22957	0.23023
90	0.25000	0.25000	0.25000	0.25000

Table VIII

$H°$	$v(H)\cos H$		
	(U)	(G)	(O)
0	1.57	0.00	0.00
5	1.57	0.34	0.64
10	1.55	1.42	1.27
15	1.52	2.20	1.46
20	1.48	2.12	1.54
25	1.42	1.92	1.56
30	1.36	1.72	1.55
35	1.29	1.50	1.51
40	1.20	1.34	1.44
45	1.11	1.16	1.34
50	1.01	1.01	1.23
55	0.90	0.85	1.10
60	0.79	0.71	0.95
65	0.66	0.58	0.80
70	0.54	0.46	0,65
75	0.41	0.34	0,49
80	0.27	0.22	0.32
85	0.14	0.11	0.16
90	0.00	0.00	0.00

cannot be rigorously evaluated (atmospheric absorption, limiting magnitude and magnitude function of meteors) and only approximate values of it are available. For the sake of comparison, we have computed k for three different assumptions:

1. for a uniform distribution of meteors, i. e. for $v(H) = \text{const.}$ (U),

2. for the theoretical distribution computed by Guth [6] for the meteors of 6.5 apparent magnitude (G),

3. for the theoretical distribution computed by Oepik [7] for observations with a 60 mm telescope of 7.5 magnifying power and 5° diameter of the field of view (0).

The second and third assumption are preferable to the first, which does not take into account the effect of atmospheric absorption; this effect considerably restricts the meteor numbers in the lowest elevations where the differences between p'_{II} and P_{II} are the largest. Both distributions (G) and (0) have been computed by assuming the Oepik's form of the luminosity function: $\frac{N_{m+1}}{N_m} = 4$ for $m < 3$ and $\frac{N_{m+1}}{N_m} = 2.5$ for $m > 3$. The values of $v(H)\cos H$ based on the above three assumptions are given in Table VIII, and the values of k satisfying the condition (47) in Table IX.

Table IX

v	$k°$		
	(U)	(G)	(O)
80 km	1.61	1.52	1.48
100 km	1.87	1.76	1.70

From Table IX it is seen that our results lead to considerably lower values of k than those derived (in an entirely different way) by Hoffmeister and Prentice. The discrepancy is mainly due to different assumptions as to the thickness of the atmospheric layer in which meteors are visible. However, the assumption of a thinner layer seems to be justified in case of telescopic work where a great majority of observations falls on extraordinary faint meteors exhibiting only short visible paths.

It may be pointed out that there are two problematical points in the derivation of formula (34) by Prentice. Firstly, it does not include any relation between inclination and depth of penetration by using uniform limits of the atmospheric layer, in which meteors are visible, for all radiant altitudes. Secondly, Prentice's procedure is valid only for the field of view centered at the zenith, which is actually rather an exception. Just in this case the conditions are least favourable for highest radiant altitudes; otherwise, a slight assymetry must arise in the distribution of radiants of observed meteors, more meteors being observed from the radiants situated behind the observer than from those situated in front of him. Both the effects indicated tend to decrease the value of $k = 6°$ in Prentice's formula.

The effect of restriction of the field of view, considered by Prentice, may be of an enhanced importance in telescopic observations, where the depth of penetration is large compared with the

size of the observed section of the atmospheric layer. However, as this effect is closely connected with the effect of angular speed, it has not been included in deriving the formulae (17), (29) based exclusively on geometrical considerations. It will be treated in paragraphs 6 and 8 together with several addidtional effects which cannot be rigorously evaluated.

6. The Possible Sources of Discrepancies between Observation and Theory

In the preceding paragraphs a simplified geometrical theory of the direction distribution has been outlined, taking into account the effects of the Earth's curvature and gravitation. However, there are some effects of different kind which may eventually sensibly influence the real distribution shown by direct observations. They are as follows:

1. *The apex—antapex streaming.* The distribution of geocentric directions of meteors is by no means isotropic being influenced by the Earth's orbital motion. A concentration of the apparent radiants in the region of the apex and a dilution in the region of the antapex must be expected.

2. *The ecliptical concentration.* If the orbits of a fract on of telescopic meteors are planetary in character, also a concentration of radiants along the ecliptic and a reduction J(1) must take place.

3. *The presence of meteor streams.* If a number of telescopic meteors forms a meteor stream, the position of its radiant must appear in the final direction distribution.

4. *The effect of the inclination.* The visibility of meteors may be correlated with their inclinations to the Earth's surface. The meteors meeting the atmosphere under smaller angles commonly exhibit longer visible trails but, owing to the smaller density gradient along the path, they may be somewhat fainter.

5. *The effect of the angular velocity.* The visibility of telescopic meteors closely depends on their angular velocity. Abnormally fast meteors may cross the field of view so quickly that the observer does not perceive them. As the angular velocity increases with the elongation of the meteor from the radiant (reaching the maximum at $\varepsilon = 90°$ and decreasing again towards the antiradiant) and with the altitude above the horizon (reaching the maximum at the zenith), in higher altitudes only those meteors are seen which are either not too distant from the radiant or sufficiently bright. An analogous selection is due to the differences in geocentric velocities of meteors coming from the apex and antapex; this selection may partially ballance the effect (1) in the case of telescopic observations.

6. *The restriction of the field of view.* The maximum surface exposed to the penetration of meteors from a given radiant is one inclined to the respective atmospheric level. This inclination increases the number of meteors visible in a restricted field of view. The effect is the more prominent the larger the angle between the direction of the meteor's motion (apart of its orientation) and the direction of view; simultaneously it is more prominent for a smaller field of view, lower altitude and greater depth of penetration. (By other words, it closely depends on the properties of the telescope used, especially its aperture and magnification.) The operation of this effect relates only to the meteors entering or leaving the field of view on its border. It must be emphasized that just these meteors move with higher angular speeds, and, as a consequence, the factors (5) and (6) are working one against another.

According to the way in which they influence the distribution of apparent directions, the six factors given above may be divided into two groups with the following characteristics:

I. The operation of the factors (1)—(3) does not depend directly on the altitude of the field of view. It is correlated with the positions of the apex (1), ecliptic (2) and active shower radiants (3), respectively; i. e. with the orbital characteristics of telescopic meteors in the Solar system.

II. The operation of the factors (4)—(6) depends almost exclusively on the altitude of the field of view, and, consequently, is symmetrical with respect to the vertical. Only in (5) the position of the apex introduces some corrections of the second order. The effects of this group bear upon the properties of visible meteor trails within the Earth's atmosphere and the instruments used for the observations.

It may be shown that the effects (1)—(3) cancel out in the main part in properly chosen and elaborated observations. If the observations are made in different nights of the year as well as in different night hours (thus providing a sufficient range of variability for the altitude of the apex and position of the ecliptic, and radically diminishing the contribution of shower meteors) the effects (1) and (2) will appear in different distribution of directions in different azimuths. However, they will not affect the composite distribution of

directions computed with respect to the altitudes but without respect to the azimuths.

In order to identify the influences of the various factors we shall examine the distribution of directions in a series of observations satisfactorily fulfilling the above conditions. At first, we shall investigate the effects (4)—(6) on the basis of the distribution of position angles of the meteors' apparent motions in different altitudes, apart of their azimuths. After comparing the actual distribution with the results of the paragraphs *3—5*, we shall pass to discuss the effect (1)—(3) so as to obtain some informations concerning the heliocentric orbits of telescopic meteors.

7. The Observations to Be Compared with the Theory

For the sake of comparison with the present theory a series of telescopic observations of meteors, carried out at the Skalnaté Pleso Observatory during the years 1947—1953, has been worked out and the real distribution of directions deduced. There are observations of 1016 telescopic meteors for which the altitudes (to nearest integer 5°) and the position angles of the apparent motion with respect to the vertical (to nearest integer 10°) have been recorded; for 527 meteors the estimates of the azimuths a e also available. As to the systematic errors, the only important could be those in the altitude on which the resulting direction distribution closely depends. There is a well-known fact that the estimates of altitudes, obtained from visual observations, are usually subjected to considerable systematic errors positive in sign. However we have wood reason to suppose that the observations in question are free of errors of that kind, as the altitudes have been estimated according to the inclination of the telescope adjusted on an altazimuth mounting. The observations cover rather uniformly different seasons of the year as well as different night hours, with a moderate selection in favour of the autumn months and evening hours. The distribution of observed meteors over the visible hemisphere (partially covered on the western side by the mountain range of Lomnický, Kežmarský and Huncovský štít) is shown in Figure 6, where the frequency of observed meteor paths is expressed in the units of the average frequency. All observations were made with the 25×100 Somet-Binar binoculars which are very efficient for a work of that kind on account of the pretty large diameter of the field (3.6°) combined with a low aperture ratio (f/4.5) and magnification ($25\times$). The mean brightness of meteors seen with this instrument is about 8^m; under most favourable conditions the limiting magnitude was 13^m for stars and 11^m for meteors.

The observers which participated in collecting the data on the meteors are given in the following table:

Table X

Observer	Period of observation	Number of meteors
M. Dzubák	1947	70
L. Kresák	1947—1953	753
M. Kresáková	1953	92
L. Mrkosová	1953	80
A. Paroubek	1953	4
R. Šáškyová	1953	9
Sum		1008

8. The Effects of Inclination, Angular Velocity, and Restriction of the Field of View

The contribution of these three factors would be taken into account by direct applying the due corrections to the probabilities p'_{II}. On the other hand, this contribution may be approximately evaluated by comparing the observed distribution of directions in different altitudes with the expected one, based on the figures of Table V.

Owing to the symmetry of the effects in question with respect to the vertical we may divide the observed meteors into two groups: those coming from above (a), i. e. moving in the position angles $\vartheta = 0°$ to 90°, or 270° to 360°, and those coming from below (b), i. e. moving in the position angles $\vartheta = 90°$ to 270°. Hence

$$P_a = 2P_I = 2P_{IV} \tag{48}$$

$$P_b = 2P_{II} = 2P_{III} \tag{49}$$

Denoting by N_a the number of meteors coming from above, by N_b the number of meteors coming from below, and by N the sum $N_a + N_b$, we have

$$N_a = NP_a \tag{50}$$

$$N_b = NP_b \tag{51}$$

The values of N, N_a and N_b deduced from the observations are given in the 2nd, 3rd and 4th column of Table XI. They are tabulated for different altitudes H graduated by five degrees (first part of the Table), and in addition for three subgroups of meteors: those of low altitudes — $H = 0°$ to 15°,

those of moderate altitudes — $H = 20°$ to $30°$, an those of higher altitudes — $H = 35°$ and more (second part of the Table). Of the meteors whose directions fall on the limits of the two regions a and b (position angle $\vartheta = 90°$ or $\vartheta = 270°$) the one half has been included into the number N_a and the other half into the number N_b, thus letting arise the fractions in the values of N_a and N_b.

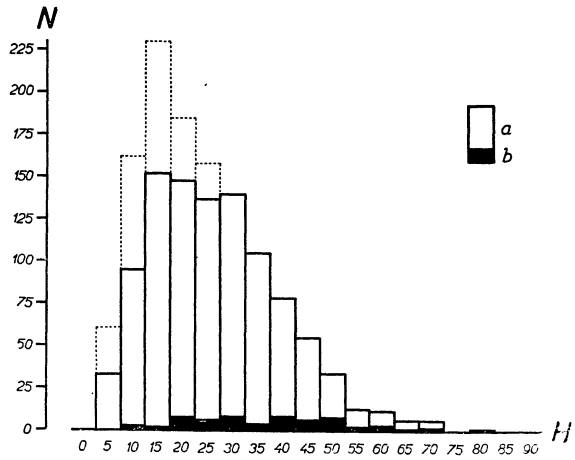

Figure 3.

A histogram of the quantities N_a and N_b, derived from the observations, is shown in Figure 3. The areas delimited by the dotted lines represent the proportional numbers of meteors falling on the section of the sky covered by terrestrial hindrances (cf. Figure 6); thus the total heights of the columns correspond to the values of $\nu(H)$ resulting from the employed method of observation. A more detailed representation of the observed distribution of directions is seen in Figure 4, where the occurence of various directions is shown in the form of three polar diagrams: A. for H ranging from $0°$ to $15°$, B. for H ranging from $20°$ to $30°$, C. for $H = 35°$ and more. The concentric circles indicate the frequencies of individual directions in terms of the average frequency. The curves have been constructed by joining the points separated in the position angle by $15°$, the frequency for each individual ϑ being computed from the interval $<\vartheta - 15°,\ \vartheta + 15°>$ without smoothing. The black areas at the bottom of the curves correspond to the numbers N_b; their progressive enlargement with increasing altitude is clearly demostrated.

In order to discover the variations of the direction distribution brought about by the effects of inclination, angular speed and restriction of the field of view, we may directly compare the observed numbers N_b with those received by inserting the values of Tables V and VII into the formulae

Table XI

$H°$	Observed			Computed					
				N_b					
	N	N_a	N_b	$v = 80$	$v = 100$	$k = 0°$	$k = 2°$	$k = 4°$	$k = 6°$
0	0	0	0	0.0	0.0	0.0	0.0	0.0	0.0
5	33	33	0	0.2	0.2	0.1	0.1	0.3	0.4
10	95	92	3	1.2	1.3	0.7	1.1	1.5	2.1
15	152	149.5	2.5	3.4	3.5	2.6	3.4	4.3	5.2
20	148	140	8	5.3	5.4	4.5	5.4	6.4	7.4
25	137	130.5	6.5	7.2	7.3	6.4	7.4	8.4	9.5
30	140	131.5	8.5	10.2	10.3	9.4	10.5	11.6	12.7
35	105	101	4	10.1	10.2	9.5	10.3	11.2	12.1
40	79	70.5	8.5	9.7	9.7	9.2	9.9	10.6	11.2
45	55	48.5	6.5	8.3	8.4	8.1	8.5	9.0	9.4
50	34	26	8	6.2	6.3	6.1	6.3	6.6	6.9
55	13	10.5	2.5	2.8	2.8	2.8	2.9	3.0	3.1
60	12	9	3	3.0	3.1	3.0	3.1	3.2	3.2
65	6	5	1	1.8	1.8	1.7	1.8	1.8	1.8
70	6	4	2	2.0	2.0	2.0	2.0	2.0	2.1
75	0	0	0	0.0	0.0	0.0	0.0	0.0	0.0
80	1	0	1	0.4	0.4	0.4	0.4	0.4	0.4
85	0	0	0	0.0	0.0	0.0	0.0	0.0	0.0
90	0	0	0	0.0	0.0	0.0	0.0	0.0	0.0
0—15	280	274.5	5.5	4.8	5.0	3.4	4.6	6.0	7.7
20—30	425	402	23	22.6	23.0	20.3	23.2	26.3	29.6
35—90	311	274.5	36.5	44.4	44.6	42.8	45.2	47.7	50.2
0—90	1016	951	65	71.7	72.6	66.4	73.1	80.1	87.5

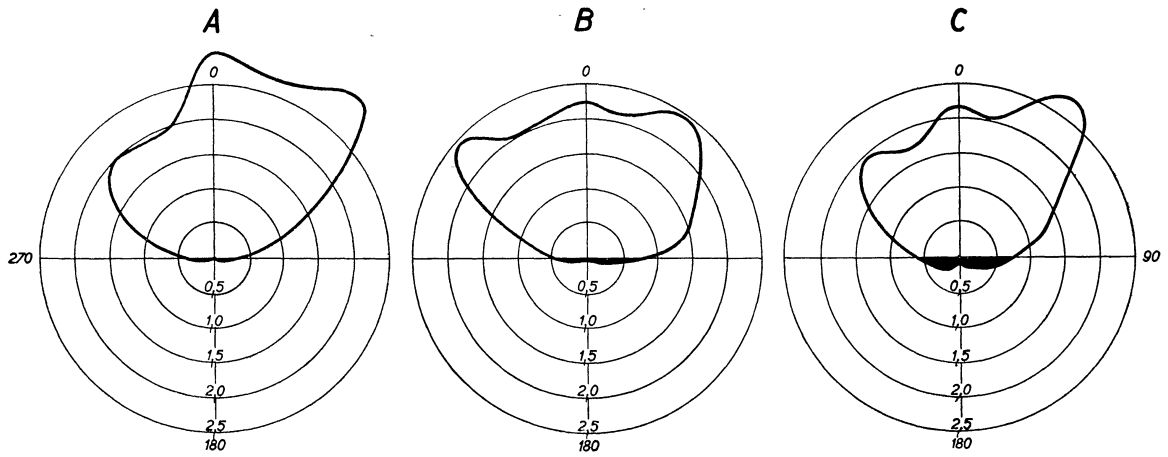

Figure 4.

(49), (51). Such comparison is shown in the Table XI which needs a particular examination.

The Table proves us that the actual distribution of direction fairly closely follows the computed one. The collected data, although containing over one thousand meteors, are not quite sufficient to permit a detailed investigation for each individual altitude; therefore the meteors have been arranged into three subgroups, approximately equally numerous, containing the lowest, moderate and higher altitudes (the division is the same as in Figure 4). The results obtained for these three subgroups and for the total of meteors are given in the lower part of the Table.

In discussing the results we must remember that due to the Law of Chance the observed values of N_b are subjected to natural uncertainties of about $\sqrt{N_b}$. Consequently, we are not able to distinguish between the suppositions which lead to numerically similar probabilities (such as p'_{II} for $v = 80$ km and $v = 100$ km). However, for the simplified formula (36) an upper limit of k may be stated at any rate, for which the agreement between observation and theory is satisfactory.

According to the last line of the Table, only the assumptions of k higher than 2° must be rejected; all other assumptions fit the observed distribution within the expected limits. There is only a little defect of N_b in the subgroup of highest altitudes, which may be perhaps connected with the effect of angular speed. In high altitudes just those meteors, whose paths are less inclined to the plane of the horizon, move with higher angular velocities, and may therefore easier escape the observation than the others. However, the defect is by no means a pronounced one, as may be clearly seen from Figure 5, where the a priori probabilities P_b (given in full line for $v = 80$ km) are shown compared with the respective a posteriori probabilities derived from the observations (indicated by the circles whose areas are proportional to the numbers of meteors included).

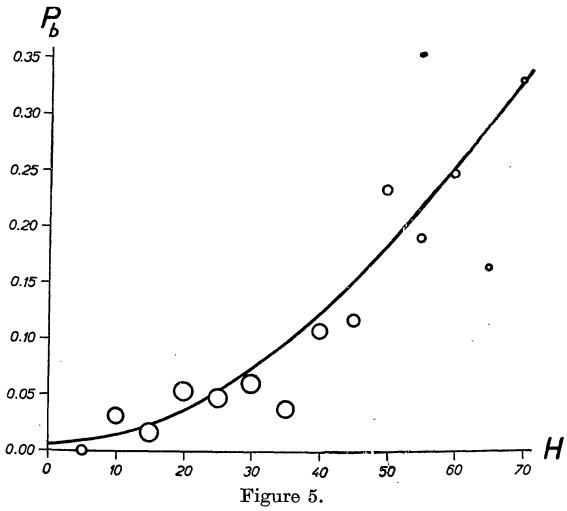

Figure 5.

In order to distinguish between the various effects treated in the present paragraph, a special procedure must be employed. It is obvious that the effect of restriction of the field of view depends on the ratio of the lengths of the meteors' visible trails to the diameter of the field of view. If the ratio drops to zero, the effect vanishes. Thus if we want to obtain the distribution of directions free of that effect, we need only to reckon up the beginnings and endings of the meteor trails, visible inside the field of view, instead of the meteors themselves, and correlate these numbers with the

Table XII

$H°$	Observed			Computed					
				N_b					
	N	N_a	N_b	$v = 80$	$v = 100$	$k = 0°$	$k = 2°$	$k = 4°$	$k = 6°$
0	0	0	0	0.0	0.0	0.0	0.0	0.0	0.0
5	39	39	0	0.2	0.3	0.1	0.2	0.3	0.5
10	87	85	2	1.1	1.2	0.7	1.0	1.4	1.9
15	99	97	2	2.2	2.3	1.7	2.2	2.8	3.4
20	116	107.5	8.5	4.1	4.2	3.5	4.2	5.0	5.8
25	79	75.5	3.5	4.1	4.2	3.7	4.3	4.8	5.5
30	89	81	8	6.5	6.5	6.0	6.6	7.4	8.1
35	54	52	2	5.2	5.2	4.9	5.3	5.8	6.2
40	41	35.5	5.5	5.0	5.1	4.8	5.1	5.5	5.8
45	35	34	1	5.3	5.3	5.1	5.4	5.7	6.0
50	16	8	8	2.9	2.9	2.9	3.0	3.1	3.2
55	7	5.5	1.5	1.5	1.5	1.5	1.5	1.6	1.6
60	10	9	1	2.5	2.5	2.5	2.6	2.6	2.7
65	4	4	0	1.2	1.2	1.2	1.2	1.2	1.2
70	4	3	1	1.3	1.3	1.3	1.3	1.4	1.4
75	0	0	0	0.0	0.0	0.0	0.0	0.0	0.0
80	0	0	0	0.0	0.0	0.0	0.0	0.0	0.0
85	0	0	0	0.0	0.0	0.0	0.0	0.0	0.0
90	0	0	0	0.0	0.0	0.0	0.0	0.0	0.0
0—15	225	221	4	3.5	3.7	2.4	3.4	4.5	5.8
20—30	284	264	20	14.7	15.0	13.2	15.1	17.2	19.3
35—90	171	151	20	25.0	25.1	24.1	25.5	26.9	28.2
0—90	680	636	44	43.3	43.9	39.7	44.0	48.5	53.3

directions. As a matter of fact, the types of visibility (i. e. the statements whether the points of appearance and disappearance lied within or outside the field of view) have been recorded for all telescopic meteors observed during the Skalnaté Pleso systematic programme.

The statistics of meteor directions compiled according to the above principle is shown in Table XII. The meaning of all quantities included is the same as in Table XI, with the single exception that the values N, N_a and N_b; correspond to the totals of the beginnings and endings of meteors observed inside the restricted field of view. We see that the agreement between observation and theory is even closer than in the preceding case (Table XI). An indirect solution for v leads to a quite reasonable value of 105 km above the Earth's surface; however, this value has no practical significance, as its probable error is very large.

What an immense number of observations would be needed for an experimental valuation of k (in the altitude of 30° about 5×10^3 meteors for the accuracy $\pm1°$ and about 5×10^5 meteors for the accuracy $\pm0.1°$; in the altitude of 60° about 2×10^4 meteors for the accuracy $\pm1°$ and about 2×10^6 meteors for the accuracy $\pm0.1°$) is well illustrated by the values of k found from the present material, which are:

$$k = -0.4 \pm 2.5° \qquad (48)$$

for the former method of elaboration (statistics of meteors) and

$$k = +2.0° \pm 3.0° \qquad (49)$$

for the latter method (statistics of the points of appearance and disappearance).

The same statistical uncertainty makes it also difficult to judge of the contributions of different secondary effects to the composite distribution of directions. Denoting by $\overline{P_b}$ the ratio $N_b : N$ (i. e. the average probability $P_{II} + P_{III}$ for the respective series of observations) we obtain the values which are given in Table XIII together with their natural uncertainties. From the Table we see that the change of $\overline{P_b}$ brought about by eliminating the restriction of the field of view is insignificant, lying within the expected limits of uncertainty. It is interesting that neglecting of this effect even somewhat diminishes the proportional number of radiants in low altitudes. It is probable that in the case of observation with instruments of usual aperture and magnification the influence of the restriction of the field of view is fully ballanced by the effect of angular velocity:

in lower altitudes it cannot be of any importance, and in higher altitudes the increased number of meteors, penetrating the observed part of the atmosphere from low situated radiants, moves so quickly that the fainter of them cannot be perceived by the observer.

Table XIII

$\overline{P_b}$ obs.		I	II
		0.064 ± 0.008	0.065 ± 0.010
$\overline{P_b}$ comp.	$v = 80$ km	0.071	0.064
	$v = 100$ km	0.071	0.064
	$k = 0°$	0.065	0.058
	$k = 2°$	0.072	0.065
	$k = 4°$	0.079	0.071
	$k = 6°$	0.086	0.078

As to the dependence of the meteors' visibility upon their inclination, the close coincidence between observed and computed values of P_b proves that there may be no marked connection at all.

The analysis of the results of observations leads to the conclusion that the computed values of the probabilities p'_{II} (Table V) fit good to the actual state and may be accepted as a reliable base for further investigations.

9. The Distribution of Geocentric Directions and its Bearing to the Orbits of Telescopic Meteors

In the preceding paragraphs we have examined the distribution of meteor directions only with respect to the vertical and parallels. If we want to gain an idea about the manner in which the directions are distributed in the space, we must refer them to a spherical system of coordinates. The use of an ecliptical system with the longitude counted from the apex or antapex would be principally the most advantageous. However in this case the conditions of the observations (first of all the non-uniform distribution of observed meteors over the sphere) would produce disturbing effects of selection which would be very difficult to eliminate. For that reason it has been found preferable to make use of the horizontal system of coordinates, in which the actual distribution of directions may be constructed most easily and reliably. Obviously, the positions of apex, antapex and ecliptic undergo continuous variations in this system, but the variations are restrained to certain regions of the sphere only, and, moreover, the range of variations may be still reduced by a proper division of the observations.

Among the observations mentioned in the 7th paragraph, for 528 meteors complete records including the azimuth, altitude and position angle of the motion were available. These records have been worked up in a similar manner to that used by Hoffmeister in his „Meteorströme" [8]. The observed paths of meteors have been prolonged backwards to meet the horizon and the frequency of the prolongations has been investigated as a function of the position in the horizontal system.

There may be a point of objection against this procedure: it consists in the fact that the effect of angular velocity has been fully neglected. The probability of a certain section of the prolongation to contain the actual radiant depends on the angular velocity of the meteor, on the distance from the point of appearance, and on the length of the prolongation from that point to the horizon. Perhaps it would be more correct to ascribe different weights to individual sections of the backward prolongations, but we have no concrete criteria for doing so. Besides, such treatment would enhance another disturbing effect, coming from the non-uniform distribution of observed meteors over the visible hemisphere.

Since this non-uniformity may play a certain rôle even in the present method of elaboration, the local distribution of observed meteors has been properly examined. The result of this examination is shown in Figure 6 in the form of an isopletal diagram. Observed meteor paths have been counted in the areas of 15×30 degrees and from these counts the frequencies of meteor paths in different points of the sky, expressed in terms of the average frequency, have been derived. The curves drawn in the Figure correspond to the interpolated values of one-, two-, and three-fold average frequency; the heavy line at the right and above, delimiting the blank area, represents the mountain range elevated above the geometrical horizon of the observatory. An increased concentration of observed paths in the altitudes $10-40°$ is plainly demonstrated as well as their relatively uniform distribution among different azimuths. The prominence of increased frequency high in the east is due to systematic observations near the radiant of the Lyrid stream during its 1953 return.

In order to obtain a statistical representation of the distribution of sporadic radiants, the following procedure has been adoptated. A chart of the hemisphere in the gnomonic projection has been drawn in a large scale, with 55 selected points sur-

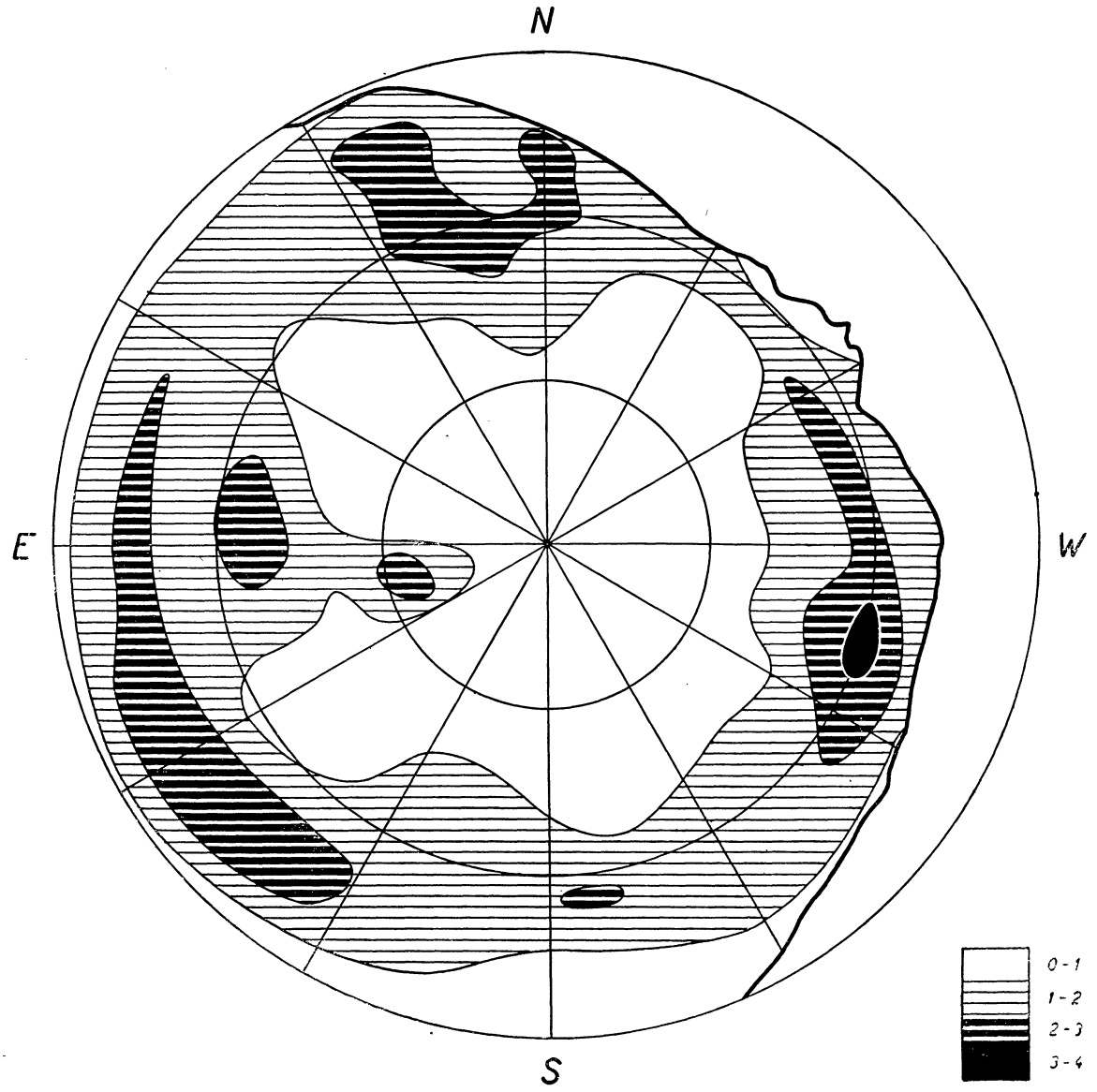

Figure 6.

rounded by circular fields 20° in diameter.* The points have been chosen so as to occupy rather uniformly the whole visible hemisphere. On a transparent sheet a cross has been drawn, bearing on the vertical arm a scale of zenithal distances, gnomonically projected. Denoting by brackets the projected lengths and by A an arbitrary constant setting the scale of the chart we have:

$$(z) = A \tan z \qquad (50)$$

For fixing the great circle arc of a meteor path in the gnomonic projection by means of the cross, the coordinates of two points are necessary. One is given approximately by the azimuth and altitude of the field of view; for the other the point of nearest approach to the zenith may be adopted with the best advantage. Its zenithal distance Z may be found by solving the equation following from the Napier rule,

$$\sin Z = \sin \vartheta \cos H \qquad (51)$$

* In the projection the fields are shown in the form of ellipses, only the lowest ones, touching the horizon, in the form of parabolas and that around the zenith in the form of a circle. The major axes of the conic sections coincide with the verticals. Obviously, the whole hemisphere cannot be represented, but on a chart restricted to the zenithal distances, say, 0° to 80°, also the intersections of the border fields can be fixed quite reliably by extrapolation.

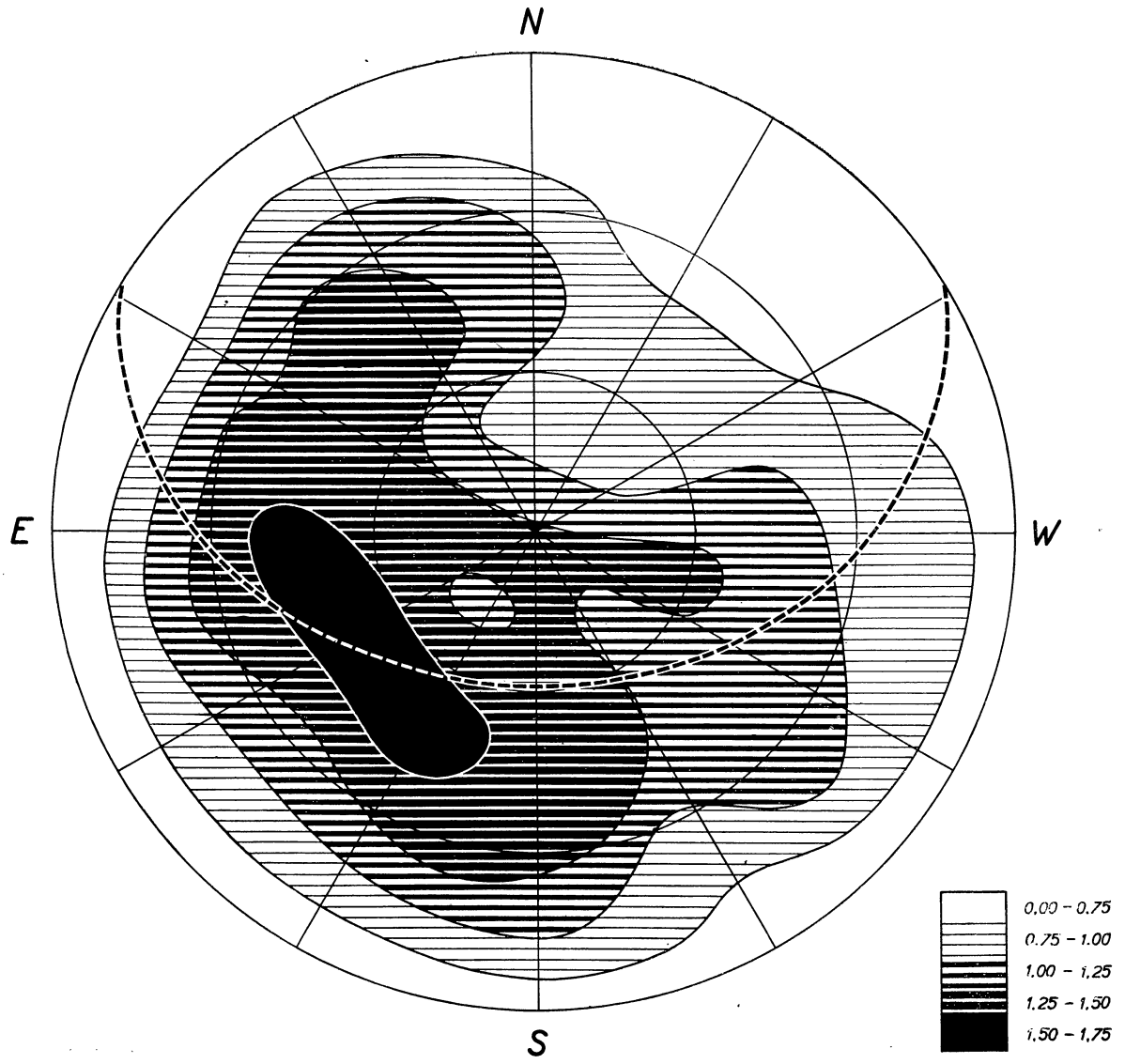

Figure 7.

in which ϑ denotes the position angle and H the altitude of the observed path (cf. Figure 1). If we lay the transparent sheet on the chart so as to let the marking of zenithal distance Z coincide with the middle point of the chart, and the other arm of the cross meet the point of horizontal coordinates a, H, all intersections of the selected fields along the backward prolongations may be easily read off. Obviously, one half of the transparent scale has to be used for $0° < \vartheta < 90°$ or $180° < \vartheta < 270°$, and the other half for $90° < \vartheta < 180°$ or $270° < \vartheta < 360°$. With the aid of this procedure all intersections occuring on the chart have been listed and counted according to the respective fields. The isopletes referring to 0.75, 1.00, 1.25 and 1.50 average frequency of prolongations have been constructed again by interpolating between the directly computed values.

The best check on the reliability of the deduced results consists in halving the material and treating the two subgroups separately and independently. As the relation of the radiants to the apex was of great interest, a division according to the declination of the apex has been adopted.

The first group contains the meteors observed at the heliocentric longitudes 315° to 45°, when the apex' declination ranges from +16.5° to +23.5°, i. e. in the neighbourhood of the apex' northern extremity. In the second group the remaining meteors have been included (apex' de-

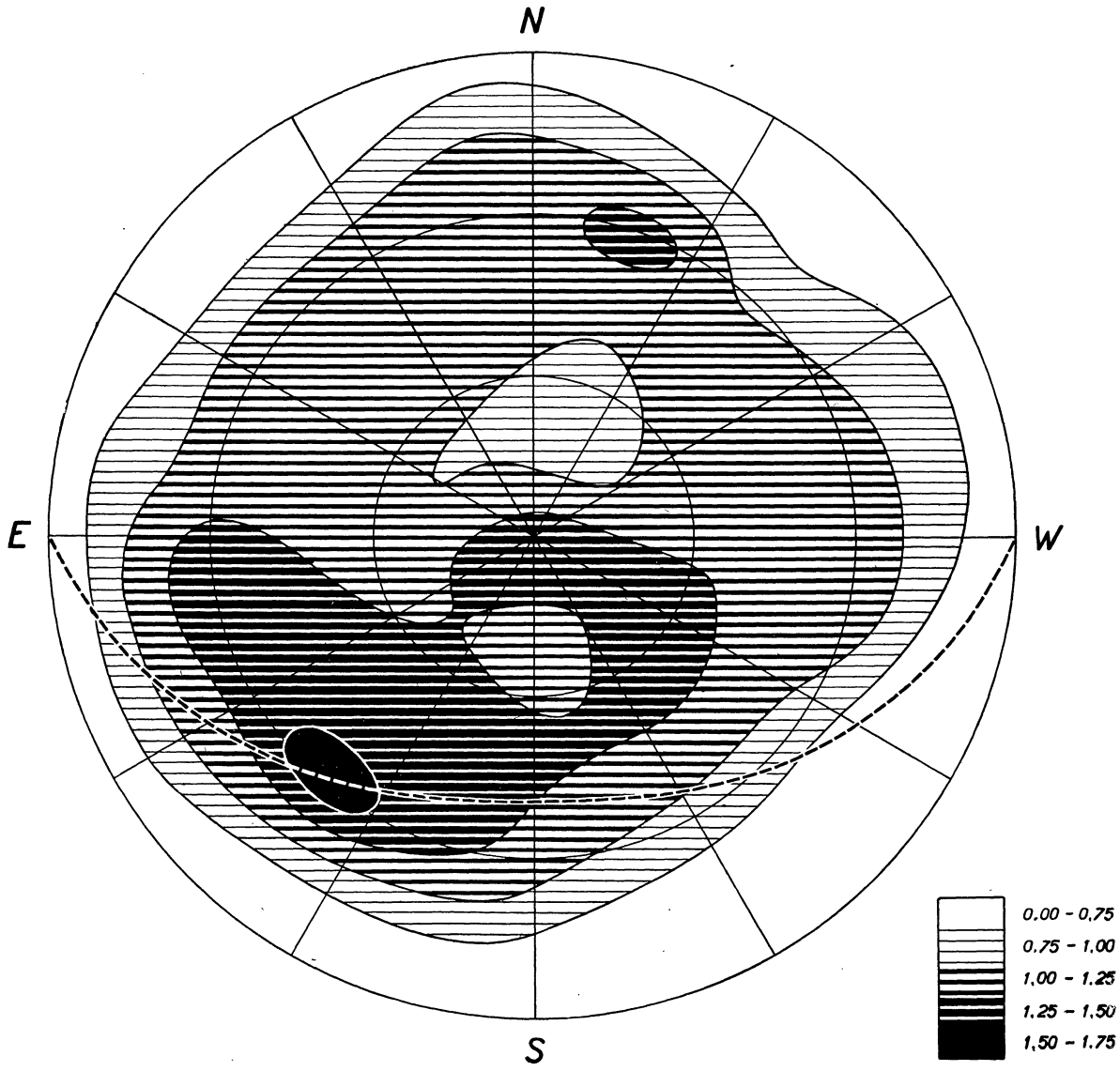

Figure 8.

clinations from $-23.5°$ to $+16.5°$). The first group consists of 248 observed meteor paths with 1992 intersections of the selected fields; the second group consists of 279 paths with 2208 intersections. On the average, 8 intersections fall on each individuall prolongation.

Isopletal diagrams of the frequencies of prolongations are shown in Figures 7 and 8. The mean diurnal path of the apex is approximately represented by the dashed line; for Figure 7 the parallel at $\delta = +20°$ has been adopted, for Figure 8 the equator. It may be noted that during the observations the apex occupied positions generally not too distant from the eastern horizon: for meteors of the first group the apex' altitudes were predominantly positive, for meteors of the second group negative.

The main outlines of the two diagrams are rather similar. In both cases the regions of densest radiant concentration are closely attached to the path of the apex, the maximum concentration approximately coinciding with the position of the apex about three o'clock after local midnight. By taking into consideration the effect of the Earth's orbital motion, we had to expect a state rather similar to that shown in the Figures. Due to the vectorial composition of the heliocentric velocities, uniformly distributed true radiants must form a non-uniform distribution of apparent radiants, showing highest concentration near the apex and a continual decline

towards the antapex. As the frequency of meteors becomes greater with increasing altitude of the radiant, the region richest on sporadic radiants is expected to lay between the apex and the zenith. It may be noted that the lack of radiants in the lowest altitudes, clearly shown on the Figures, is a little different in the nature but the same in the original reason: it is due to the fact that the backward prolongations of meteors, moving predominantly from above and appearing predominantly in moderate altitudes, avoid the region below the field of view.

The effect of the Earth's orbital motion simultaneously stipulates the predominancy of an apparent east-west streaming of the meteors. This may be shown on a polar diagram of directions, analogous to those of Figure 3. Reckoning the position angles directly south of the prime vertical and retrogadely north of it i. e. adding the number of position angles ϑ in the azimuths 270° to 90° to that ot the position angles 360° — ϑ in the azimuths 90° to 270°) we obtain a sensibly as-symetrical distribution of directions. The auxiliary mirror-like dotted curve in Figure 9 shows how much the eastern directions actually prevail over the western ones.

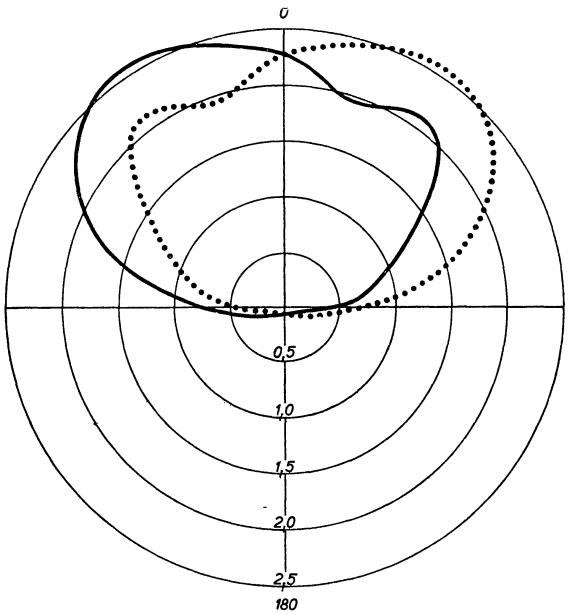

Figure 9.

There is still another point of interest in the course of the isopletes in Figures 7 and 8, which gives evidence of a peculiar arrangement of the telescopic meteor orbits within the Solar system: it is the relation of the radiants to the ecliptic. If the inclinations of the orbits were distributed at random, the apex-concentration would be the single substantial feature on the diagram. On the contrary, in case as the orbital planes were more numerous near the fundamental plane of the Solar system, an additional concentration of the radiants near the ecliptic would appear. We see that just this is the case; it may be demonstrated on two facts, shown independently both in Figures 7 and 8:

1. The region of highest frequency of the path prolongations does not lie between the apex and the zenith but farther southwards, close to the ecliptic.

2. The region around the antihelion point (and even farther towards the antapex) presents higher frequency than the region around the north pole of the ecliptic, although its distance from the apex is the same and the distance from the zenith even larger. The effect is clearly seen especially in Figure 7, where the low frequency in the NW quadrant (containing the pole of the ecliptic) surprisingly contrasts with the high frequency in the SW quadrant (pierced by the antapex and later by the antihelion point during their night's motion).

Hence the bearing of the orbits of telescopic meteors to the plane of the ecliptic is clearly demonstrated. It is readily explicable by the conception that a part of telescopic meteors moves in orbits similar to those of some minor planets or ecliptical meteor streams. This conception is moreover supported by the fact that the apex-concentration seems to be comparatively moderate, which gives evidence of direct motions prevailing over retrograde.

10. On the Presence of the Hypothetical Antihelion Component

Some twenty-five yeras ago Oepik [9] has investigated the direction distribution of telescopic meteors on the base of a series of systematic observations carried out at the Tartu University Observatory. He found a rather peculiar distribution characterized by a marked antihelion streaming overlapping the much less pronounced apex—antapex component. Oepik did not try to give any interpretation of this phenomenon, attaching only the following remarks to his announcement: "... Though there are several factors, such as zenithal attraction, which may slightly favour directions toward $P = 270°$ for the North Pole area, these are utterly insufficient to explain the pheno-

menon. The conclusion is that there seems to exist a marked apparent streaming of meteors approximately toward the Sun. This streaming appears to represent a general statistical property of the meteors. Different seasons of the year equally reveal this phenomenon . . ." On the basis of similar but not so numerous telescopic observations, carried out in 1941 at the Stalinabad Observatory, this result has been confirmed by Bacharev [10].

It may be demonstrated that this streaming is only a consequence of observational selection and that the Oepik's and Bacharev's results do not contradict the present theory. It is substantial that all observations concerned have been made in the same region of the sky, i. e. in the North Pole area. We shall now discuss Oepik's data, which are more detailed and comprehensive; as the Tartu Observatory is located at $+58°4$ northern latitude, they refer to a point whose invariable horizontal coordinates are $a = 180°$, $H = +58°4$.

Oepik reckons the position angle in the same direction as we do, but he puts the beginning into the direction apex—antapex. Our position angle ϑ, fixed with respect to the vertical, coincides with the Oepik's position angle P at the upper culmination of the apex; otherwise the two systems rotate one with respect to another in a period differing but little from a Mean Solar Day. At local midnight the following relation holds between ϑ and P:

$$\vartheta = P + 90° + \varepsilon \tag{52}$$

where ε is a variable term depending on the eccentricity of the Earth's orbit and on the inclination of the ecliptic. As it oscillates during the year only between the limits $<-6°, +6°>$, it may be neglected in the first approximation.

According to the Table V, in the case of an isotropic distribution of geocentric directions in the altitude $H = 58.4°$ about 37.9% of the meteors would have their apparent motions in the position angles $\vartheta = 0°$ to $90°$, 12.1% in $\vartheta = 90°$ to $180°$, 12.1% in $\vartheta = 180°$ to $270°$, and 37.9% in $\vartheta = 270°$ to $360°$. Thus were the observations distributed uniformly among different day- and night-hours, the distribution in P would be also uniform. In each other case a non-uniform distribution must arise, with a maximum corresponding to the highest frequency of $\vartheta = 0$; the maximum would be the sharper the more markedly the observations would be concentrated around a certain hour.

From Oepik's results (l. c. Table 3) we see that the mean moment of apparition of the meteors was about 10 or 15 minutes before local midnight, 70% of meteors being observed between 22^h and 2^h Mean Solar Time. Consequently, in the distribution of directions a pronounced maximum must appear at $P = 270°$, which direction frequently differed but little from the direction from the zenith ($\vartheta = 0°$). Taking into account the contribution of the actual apex—antapex streaming, produced by the orbital motion of the Earth, a secondary maximum at $P = 0°$ is to be expected.

We see that the qualitative agreement between observation and theory is excellent. However, to obtain a quantitative check as well, we shall apply the results of Table V directly to those given by Oepik. We shall retain Oepik's division into observations before and after midnight, and put $\vartheta = P + 120°$ for the former group, $\vartheta = P + 60°$ for the latter group, and $\vartheta = P + 90°$ for the total. Due to the fact that the actual conditions differ in the individual cases from those expressed by the mentioned three equations, the probabilities p' from Table V have to be a little smoothed; instead of $p'_{\mathrm{I}} = p'_{\mathrm{IV}} = 0.379$, $p'_{\mathrm{II}} = p'_{\mathrm{III}} = 0.121$ we put:

$$p'_{\mathrm{I}} = p'_{\mathrm{IV}} = 0.37 \tag{53}$$

$$p'_{\mathrm{II}} = p'_{\mathrm{III}} = 0.13 \tag{54}$$

for the two subgroups where the dispersion of the values $\vartheta - P$ is reduced by the division according to the time of apparition, and

$$p'_{\mathrm{I}} = p'_{\mathrm{IV}} = 0.36 \tag{55}$$

$$p'_{\mathrm{II}} = p'_{\mathrm{III}} = 0.14 \tag{56}$$

for the total of observations.

In the Table XIV Oepik's results are shown compared with the respective theoretical values. N_o denotes the observed number of meteors whose position angles fall within the indicated limits of P; N_c is the expected number derived with the aid of (53)—(56) for an isotropic distribution of geocentric directions. From the ratios $\frac{N_o}{N_c}$ we see that after applying the reduction for the apparent distribution of directions in the given altitude, the antihelion component entirely vanishes. Now the extreme values of $\frac{N_o}{N_c}$ occur near $P = 0°$ and reveal the actual apex-antapex streaming. Quantitatively, about three times as much radiants lie in the right ascension of the apex as in the right ascension of the antapex. Even a little more ra-

diants appear east of the apex than west of it (especially in the morning hours), but the difference is not significant. Hence we may conclude that the secondary apex—antapex component represents the only real streaming of meteors to be found in the Tartu observations, the apparent primary antihelion component being entirely accounted for the special circumstances of these observations.

Table XIV

Observations before midnight:

ϑ	P	N_o	N_c	$\frac{N_o}{N_c}$
0— 90	240—330	124	98	1.27
90—180	330— 60	61.5	35	1.76
180—270	60—150	37.5	35	1.07
270—360	150—240	45	98	0.46

Observations after midnight:

ϑ	P	N_o	N_c	$\frac{N_o}{N_c}$
0— 90	300— 30	73	69.5	1.05
90—180	30—120	37.5	24.5	1.53
180—270	120—210	12.5	24.5	0.51
270—360	210—300	65	69.5	0.94

All observations:

ϑ	P	N_o	N_c	$\frac{N_o}{N_c}$
0— 90	270—360	187	164	1.14
90—180	0— 90	100.5	64	1.57
180—270	90—180	51.5	64	0,80
270—360	180—270	117	164	0,71

Before closing this paragraph it may be emphasized that the proof of the apex—antapex streaming in the Tartu observations is of considerable importance also for judging of the effect of angular velocity. Various authors claim that owing to the magnification of the angular velocity by the telescope only those meteors may be seen telescopically whose radiants lie in the close vicinity of the field of view (cf [11]). If this were true, no marked apex—antapex streaming could be revealed in the Tartu observations, having been made not only in great angular distances from the ecliptic but also in high altitude (i. e. in a relatively short distance from the observer) and with a telescope of no extraordinary low magnifying power (9.2-fold). It is unacceptable that the meteors of great radiant elongations have not been recorded due to the effect of angular velocity. Were the concentration of radiants to the apex so pronounced that just in a small area around the field of view differences in radiant frequencies of the order 3 : 1 in favour of the directions towards the antapex could appear, then the abundance of telescopic meteors observed near the antapex would be absolutely incomparable with the abundance near the apex. The observations made at Skalnaté Pleso in various elongations from the apex prove that this is not the actual case. Hence we are driven to conclude that the telescopic meteors are collected from radiants distributed over the whole visible hemisphere, and that the effect of angular velocity plays no important rôle, except perhaps for the observations of faintest meteors made in high altitudes with a telescope of considerable magnifying power.

11. The Identification of Shower Meteors and Testing the Activity of Meteor Streams

The importance of this problem for the investigations of the origin and evolution of meteor streams has been pointed out just in the introductory remarks to the present paper. The considerations of the preceding paragraphs have shown that, apart of the apex—antapex component, the distribution of directions following from the a priori probabilities of Table V agrees well with the actual distribution valid for the sporadic background. The occurence of a meteor shower will obviously alter this distribution during the period of perceptible activity: an enhanced number of meteors will move in the direction from the shower's radiant.

The investigation of a given meteor stream by telescopic observations may be divided into two main tasks:

I. The verification of the existence of the shower in the range of faintest meteors and the derivation of the curve of activity.

II. The derivation of the position of the radiant point or, if possible, the construction of the radiant area formed by the cosmic spread of invidual orbits.

For solving the former task it is most advantageous to arrange the observations so as to let the direction from the radiant coincide with the direction to the zenith, and to make the observations at moderate altitudes of the radiant. In this case the influence of the shower meteors on the com-

posite direction distribution will be most efficient, and even a very low number of meteors will suffice for establishing the shower's activity. For solution of the latter task we may use most conveniently those meteors, whose apparent path prolongations include approximately right angles. Besides we must not forget that the dispersion of individual radiants of telescopic shower meteors will be probably large, and that a diffused radiation area of several degrees in diameter has to be expected in most cases. This fact would favour observations in the areas far remote from the radiant point, where the identification of shower meteors according to their directions would be easier. On the other hand, in the case of observations near at the radiant, the low angular velocity of the shower meteors would represent an additional criterion on the adherence to the stream, and the directions could be fixed much more precisely.

The above considerations enable us to develop a particular method for telescopis observations of meteor showers, which seems to be most advantageous for the purpose. For the explanation of this method consult Figure 10.

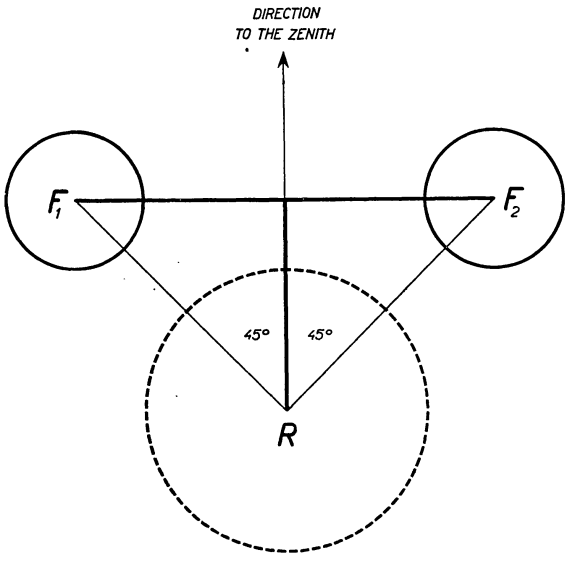

Figure 10.

Simultaneous or alternate observations in two selected fields are suggested, situated both in the same altitude aslant and above of the radiant, one (F_1) to the left and the other (F_2) to the right of it. Let us denote by a_R, h_R the horizontal coordinates of the mean apparent radiant, by a_1, h_1 those of the centre of F_1, and by a_2, h_2 those of the centre of F_2; further by D the maximum expected diameter of the radiation area and by d the diameter of the field of view. Then we obtain for the horizontal coordinates of the middle points of the two fields the following approximate relations:

$$a_1 = a_R - \frac{1}{2}(D + d)\sec\left[h_R + \frac{1}{2}(D + d)\right] \quad (57)$$

$$h_1 = h_R + \frac{1}{2}(D + d) \quad (58)$$

$$a_2 = a_R + \frac{1}{2}(D + d)\sec\left[h_R + \frac{1}{2}(D + d)\right] \quad (59)$$

$$h_2 = h_R + \frac{1}{2}(D + d) \quad (60)$$

For permanent cometary streams the assumption $D = 10°$ seems to be reasonable; in this case for observations with ordinary instruments the term $\frac{1}{2}(D + d)$ equals to about 6° to 8°. The formulae (57)—(60) will be practically sufficient for observations made anywhere except the region around the zenith. The tollerance is dependent upon the quantity $(D + d)$ and may be measured by the amount by which the section of the parallel, joining the centres of F_1 and F_2, deviates from a great circle arc. If simultaneous watches of F_1 and F_2 by two observers cannot be realized, the fields are to be alternated in such way as to record equal numbers of possible shower meteors in both of them Then the prolongations may be readily arranged into pairs, intersecting approximately perpendicularly, and the shape and size of the radiation area may be estimated with the least difficulty. Moreover, since the directions of the shower meteors fall in F_1 into the IInd quadrant and in F_2 into the IIIrd quadrant exclusively, the reality of the shower is apt to be established by directly applying the Law of Chance to the numerical values of Table V. For the suggested method of observation, the tabulated probability p'_{II} is namely equivalent with the a priori probability, that the direction of a given sporadic meteor will fall into the same quadrant as that of the shower meteors.* Suppose n meteors have been recorded during the observation, m of them moving from the IInd quadrant at F_1 or from the IIIrd quadrant at F_2. The a priori probability $P(m, n)$ of this event in a night without any shower activity is given by the Binomial Law

$$P(m,n) = \frac{n!}{m!\,(n-m)!}\,p^m\,(1-p)^{n-m} \quad (61)$$

* For the sake of abbreviation we shall replace the sign p'_{II} by p in the following formulae.

and the a priori probability $P'(m, n)$ of m or more sporadic meteors, moving in the indicated direction, by

$$P'(m, n) = \sum_{i=m}^{i=n} P(i, n) =$$

$$= \sum_{i=m}^{i=n} \frac{n!}{i!\,(n-i)!}\, p^i (1-p)^{n-i} \qquad (62)$$

Substituting the observed values m, n and the computed value of p (taken from the Table V with the argument H corresponding to the mean of h_1, h_2 during the observation), and figuring out $P'(m, n)$, we may ascertain whether the assumption of the shower activity is necessary for explaining the observed distribution of directions. As a matter of fact, the criterion is somehow conventional, like other criteria based on the Law of Chance. Generally, the value $P'(m, n) = 0.1$ may induce a rather serious suspection that the shower is actually active; by the result $P'(m, n) = 0.01$ the activity may be established beyond doubt. Obviously, in a long series also such observations will appear here and there, for which our conclusion will be erroneous. However, this uncertainty cannot influence the general character of the results as to the presence of telescopic meteors in different meteor streams.

In case that the data are extensive enough, also the frequency of shower meteors may be roughly estimated. In many cases the relation of a given meteor to the shower will be evident, or at least highly probable, just on account of its low angular velocity, eventually even combined with a typical appearance. However, apart of that the frequency of the shower in terms of the frequency of sporadic meteors f may be expressed, using the conception of the mathematical expectation, in the following form:

$$f = \frac{m}{n-m}(1-p) - p \qquad (63)$$

or after applying the approximate reduction to zenithal frequencies f_z:

$$f_z = \left(\frac{m}{n-m}(1-p) - p\right) \operatorname{cosec} h_r \qquad (64)$$

It must be warned against using formulae (61), (62) unless a sufficient number of recorded meteors is available. The formulae are practically useless if either m or $n - m$ is less than three. To avoid this disadvantage, longer observations with as efficient instruments as possible (e. g. wide angle binoculars of a sufficient diameter) are advocated. Combination of observations on several subsequent nights is suitable for a more reliable estimate of both $P'(m, n)$ and f, unless the shower activity undergoes too rapid variations. Otherwise simultaneous observations by two or more observers—watching eventually more pairs of fields defined by different assumptions of D in (60) so as to do not overlap—are preferable.

For the convenience of observers formula (62) has been evaluated for three different altitudes ($H=20°$, $H = 40°$ and $H = 60°$), n ranging from 1 to 20 and $P'(m, n) > 5 \times 10^{-5}$. The results are tabulated below: it is seen that in low altitudes just two or three meteors, moving in the required direction, are entirely sufficient for proving the shower's activity. However, in these regions the brightness of the meteors is decreased by their distance from the observer and atmospheric extinction, and care must be taken to do not restrict the data to meteors of considerable zenithal magnitudes. It is desirable to do not includeinto n and m meteors brighter than a given limiting value, and to state the investigated range of zenithal magnitudes in each case.

An objection may be made against using the Tables XV—XVII. It consists in the fact that they are based on the formulae (59), (60) in which for p the standard values of Table V have been adopted. However, as we have shown in the 9th and 10th paragraph, the standard distribution of directions agrees with the actual one only if the observations

Table XV
$H = 20°$

n	m				
	1	2	3	4	5
1	0.02	—	—	—	—
2	0.04	0.0003	—	—	—
3	0.05	0.0010	0.0000	—	—
4	0.07	0.002	0.0000	0.0000	—
5	0.09	0.003	0.0001	0.0000	0.0000
6	0.10	0.005	0.0001	0.0000	0.0000
7	0.12	0.006	0.0002	0.0000	0.0000
8	0.13	0.008	0.0003	0.0000	0.0000
9	0.15	0.011	0.0005	0.0000	0.0000
10	0.2	0.013	0.0006	0.0000	0.0000
11	0.2	0.02	0.0008	0.0000	0.0000
12	0.2	0.02	0.0011	0.0000	0.0000
13	0.2	0.02	0.0015	0.0001	0.0000
14	0.2	0.03	0.002	0.0001	0.0000
15	0.2	0.03	0.002	0.0001	0.0000
16	0,3	0.03	0.003	0.0002	0.0000
17	0.3	0.04	0.003	0.0002	0.0000
18	0.3	0.04	0.004	0.0003	0.0000
19	0.3	0.05	0.005	0.0003	0.0000
20	0.3	0.05	0.005	0.0004	0.0000

Table XVI
$H = 40°$

n	m						
	1	2	3	4	5	6	7
1	0.06	—	—	—	—	—	—
2	0.12	0.004	—	—	—	—	—
3	0.2	0.011	0.0002	—	—	—	—
4	0.2	0.02	0.0009	0.0000	—	—	—
5	0.3	0.03	0.002	0.0001	0.0000	—	—
6	0.3	0.05	0.004	0.0002	0.0000	0.0000	—
7	0.4	0.06	0.007	0.0004	0.0000	0.0000	0.0000
8	0.4	0.08	0.010	0.0008	0.0000	0.0000	0.0000
9	0.4	0.10	0.015	0.0014	0.0001	0.0000	0.0000
10	0.5	0.12	0.02	0.002	0.0002	0.0000	0.0000
11	0.5	0.14	0.03	0.003	0.0003	0.0000	0.0000
12	0.5	0.2	0.03	0.005	0.0005	0.0000	0.0000
13	0.6	0.2	0.04	0.007	0.0007	0.0000	0.0000
14	0.6	0.2	0.05	0.009	0.0011	0.0001	0.0000
15	0.6	0.2	0.06	0.011	0.0015	0.0002	0.0000
16	0.6	0.3	0.07	0.014	0.002	0.0003	0.0000
17	0.7	0.3	0.08	0.02	0.003	0.0004	0.0000
18	0.7	0.3	0.09	0.02	0.004	0.0005	0.0001
19	0.7	0.3	0.11	0.03	0.005	0.0007	0.0001
20	0.7	0.4	0.12	0.03	0.006	0.0010	0.0001

Table XVII
$H = 60°$

n	m									
	1	2	3	4	5	6	7	8	9	10
1	0.13	—	—	—	—	—	—	—	—	—
2	0.2	0.015	—	—	—	—	—	—	—	—
3	0.3	0.04	0.002	—	—	—	—	—	—	—
4	0.4	0.08	0.007	0.0003	—	—	—	—	—	—
5	0.5	0.12	0.02	0.0012	0.0000	—	—	—	—	—
6	0.6	0.2	0.03	0.003	0.0002	0.0000	—	—	—	—
7	0.6	0.2	0.05	0.007	0.0006	0.0000	0.0000	—	—	—
8	0.7	0.3	0.07	0.012	0.0013	0.0001	0.0000	0.0000	—	—
9	0.7	0.3	0.10	0.02	0.003	0.0003	0.0000	0.0000	0.0000	—
10	0.7	0.4	0.12	0.03	0.005	0.0006	0.0000	0.0000	0.0000	0.0000
11	0.8	0.4	0.15	0.04	0.008	0.0011	0.0001	0.0000	0.0000	0.0000
12	0.8	0.5	0.2	0.06	0.012	0.002	0.0002	0.0000	0.0000	0.0000
13	0.8	0.5	0.2	0.07	0.02	0.003	0.0005	0.0000	0.0000	0.0000
14	0.9	0.5	0.3	0.09	0.02	0.005	0.0008	0.0001	0.0000	0.0000
15	0.9	0.6	0.3	0.11	0.03	0.008	0.0014	0.0002	0.0000	0.0000
16	0.9	0.6	0.3	0.14	0.04	0.011	0.002	0.0003	0.0000	0.0000
17	0.9	0.7	0.4	0.2	0.06	0.015	0.003	0.0006	0.0001	0.0000
18	0.9	0.7	0.4	0.2	0.07	0.02	0.005	0.0009	0.0001	0.0000
19	0.9	0.7	0.4	0.2	0.08	0.03	0.007	0.0014	0.0002	0.0000
20	0.9	0.7	0.5	0.2	0.10	0.03	0.009	0.002	0.0004	0.0001

are uniformly distributed in different azimuths. In case of observations in a particular field, an enhancement of directions towards the antapex takes place. However, this objection is not so serious as it looks like at first glance. True, according to the Tartu observations the directions towards the antapex are enhanced by a factor of about 1.5 and those towards the apex reduced by a factor of about 0.5, but the observations in two fields, letting the direction from the radiant coincide with two different directions 90° apart in the fixed ecliptical system, makes this irregularity much less important. Perhaps only for the observations near the vertical circle joining the apex with the antapex it should be regarded.

The rapid changes of p with changing H indicate that a carefull estimate of the altitudes $h_1 = h_2$ is to be prefered to taking into account the apex—antapex component. Just an error in the altitude of several degrees may overbalance the effect of the apex—antapex streaming. Therefore it cannot be recommended to use extraordinary

long observations: the rate of $\frac{dh}{dt}$ is decisive for the tollerance in each particular case. For the same reason the method may be employed with less difficulties in higher geographical latitudes than in the lower ones.

The pronounced dependence of $P'(m, n)$ upon p makes it inconvenient to derive the particular values of $P'(m, n)$ by interpolating between the three round altitudes H given in the headings of Tables XV—XVII. For the sake of a simpler and more dependable interpolation Figure 11 has been designed, presenting the correlation between m, n, and H for $P'(m, n) = 0.1$, $P'(m, n) = 0.01$, and $P'(m, n) = 0.001$. The figure may be employed for a quick ascertainment whether the shower is present or not, before applying (62) and (63) for a rigorous solution.

The use of the Tables XV—XVII and the Figure 11 is illustrated by the following example. During an observation at the mean altitude of 45°, performed by the suggested method, 10 meteors have been recorded, 4 of them coming from the quadrant where the radiant of the stream is situated. An inspection of Table XVI and XVII shows that $P'(m, n) = 0.002$ for $H = 40°$, and $P'(m, n) = 0.03$ for $H = 60°$. In Figure 11 it is read off that for the altitude $H = 45°$ $P'(m, n)$ is only a little less than 0.01. Hence the presence of an active radiant is confirmed and a rough estimate of the frequency according to (63) may be attempted. With the aid of Table V we obtain $f = 0.5$ and (for $h_r = 38°$) $f_z = 0.8$ of the sporadic background.

12. Conclusions

1. A close dependence between the position in the horizontal system of coordinates and the apparent distribution of meteor directions has been pointed out, which surpasses all other factors entering the statistics of directions of telescopic meteors, such as instrumental and physiological effects, influence of the Earth's motion, attraction and shape, or arrangement of meteor orbits within the solar system.

2. From geometrical considerations a standard direction distribution has been derived and confirmed by direct observations. Corrections for the Earth's curvature and attraction have been deduced and evaluated.

3. The improved empirical formulae for deriving the zenithal hourly rates of meteor showers have been examined on the basis of the present theory. It has been found that only smaller departures from the cos z-law than those commonly indicated may be admitted for the telescopic observations.

4. The direct observations show that there is no significant correlation between the inclination of the meteor path to the encountered atmospheric layers, and its visibility.

5. It has been demonstrated that for an ordinary telescope suitable for the meteor work (4-inch with a 25-fold magnifying power and 3.6° diameter of the field) the selection due to the restriction of the field of view is approximately counterbalanced by the selection due to the differences in angular velocities. As a consequence, the instrumental and physiological effects on the direction distribution may be safely neglected in the first approximation.

6. It has been shown that even with the 25-fold magnification the effect of angular velocity is not so significant as to allow to observe the meteors in the region around the radiant only.

7. The derivation of the standard direction distribution made it possible to trace various irregularities, coming from the anisotropic distribution of meteor directions with respect to the Earth. The apparent apex—antapex streaming, resulting from the Earth's orbital motion, has been clearly demonstrated by the observations. Besides, a concentration of the telescopic meteor orbits to the ecliptic has been found which, together with the indicated prevalence of direct motions over retrograde, favours of the opinion that a fraction of telescopic meteors moves in orbits similar to those of some minor planets or ecliptical meteor streams.

8. The apparent antihelion streaming, found by Oepik and Bacharev, has been explained by the operation of an effect of selection.

9. A particular method for telescopic observations of meteor showers has been developed, which enables to confirm the presence, and estimate the abundance, of telescopic meteors in different streams, even when the radiant is considerably diffuse. The method is designed so as to make it possible to estimate simultaneously the size and shape of the radiation area. In connection with it special tables have been compiled for evaluating the probability as to whether a radiant is telescopically active or not.

*

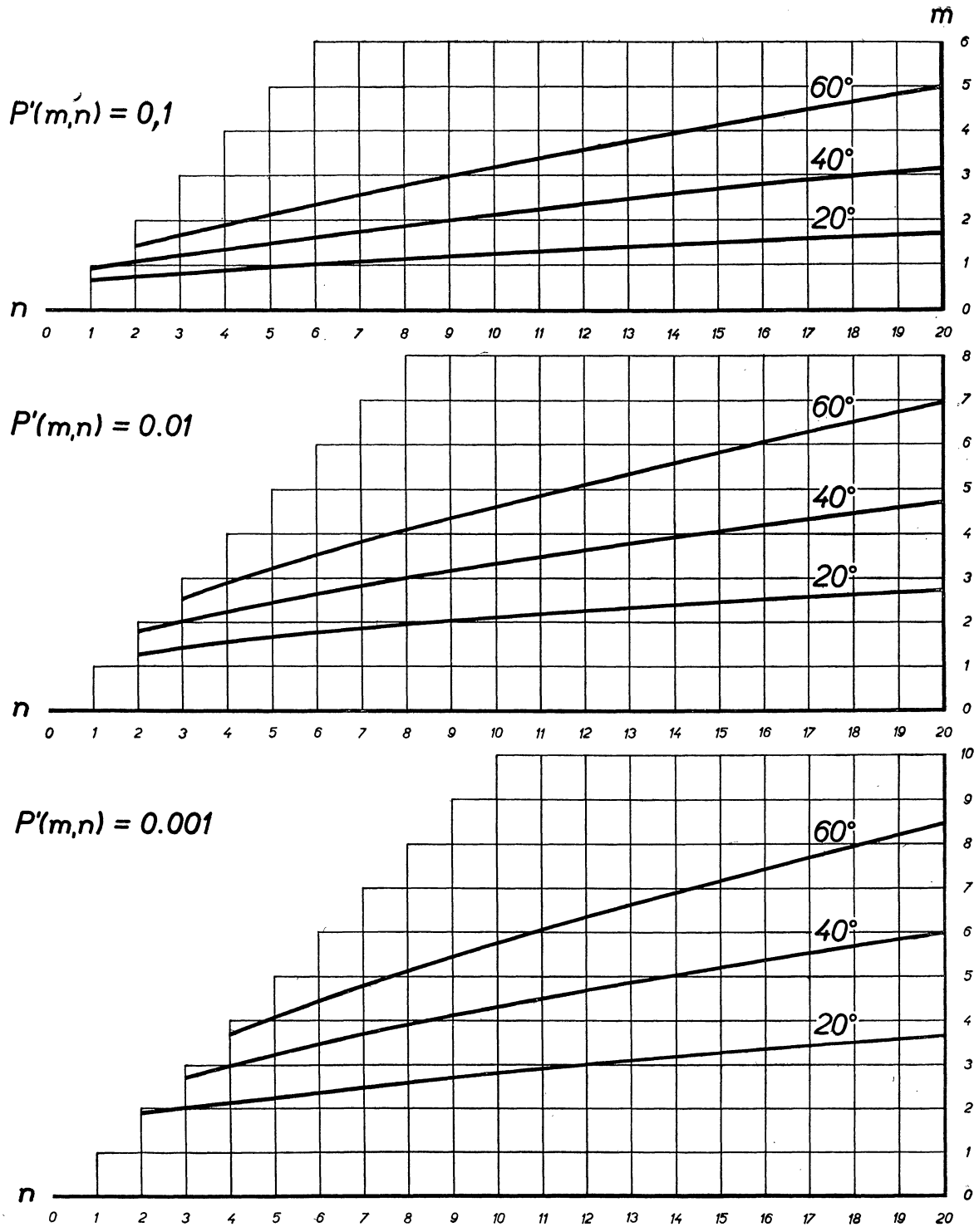

Figure 11.

My sincere thanks are due to Dr. V. Guth, Corresponding Member of the Slovak Academy of Sciences and Director of the Observatory, for his valuable advices and criticism which have facilitated the preparation of the present paper, to my wife for her helpful cooperation in arranging and reducing the observational data and to all members of our institute who have contributed to the collection of the data on telescopic meteors.

REFERENCES

[1] E. Oepik, Publications de l'Observatoire Astronomique de l'Université de Tartu, XXVII, № 2, p. 4 (1930).
[2] I. S. Astapovič, Astronomičeskij Žurnal Akademii Nauk SSSR, XII, № 1, p. 69 (1935).
[3] D. W. R. McKinley, The Astrophysical Journal, 113 № 2, p. 250 (1951).
[4] C. Hoffmeister, Astronomische Abhandlungen, IV, № 5, p. 8 (1922).
[5] J. P. M. Prentice, The Journal of the British Astronomical Association, 63, № 5, p. 176 (1953).
[6] V. Guth, Private communication.
[7] E. Oepik, Harvard College Observatory Bulletin № 879, p. 6 (1930).
[8] C. Hoffmeister, Meteorströme, p. 57, Leipzig (1948).
[9] E. Oepik, Publications de l'Observatoire Astronomique de l'Université de Tartu, XXVII, № 2, p. 7 (1930).
[10] A. M. Bacharev, Meteoritika, № VII, p. 81 (1950).
[11] C. P. Olivier, Meteors, p. 154, Baltimore (1925).

Л. КРЕСАК

РАСПРЕДЕЛЕНИЕ НАПРАВЛЕНИЙ ТЕЛЕСКОПИЧЕСКИХ МЕТЕОРОВ

В последнее время обращают все больше и больше внимания на мельчайшие твердые метеорные частицы и на их положение в солнечной системе. Точные фотографические измерения положения и скорости метеоров, которые в настоящее время могут дать нам единственные более подробные сведения о гелиоцентрических орбитах этих тел, ограничиваются практически частицами с массами порядка 10^{-2}—10 граммов. Массы менее 10^{-2} граммов относятся к слабо видимым и телескопическим метеорам, которые являются естественным переходом к невидимым частицам метеорной пыли. Последние исследования — произведенные различными независящими друг от друга способами — показывают, что на долю невидимой мельчайшей пыли приходится более значительное количество попадающей на Землю массы, чем на долю видимых метеоров. Необходимо учитывать, что наши сведения об орбитах этих тел являюся очень ненадежными, и аналогия с яркими метеорами не представляется обоснованной.

К самым актуальным вопросам метеорной астрономии относится вопрос, содержаются ли такие мельчайшие частицы метеорной пыли в различных метеорных потоках, и если да, то в каком количестве и расположении. С точки зрения образования и развития метеорных потоков особого внимания заслуживают два вопроса, решение которых надо искать в области телескопических метеоров. Первым вопросом является зависимость рассеяния орбит от величины метеоров, которая может дать известное представление о распределении импульсов между метеорами при их отделении от материнской кометы (или же при другом процессе образования), а следовательно и об условиях образования потока. Вторым вопросом является определение систематического изменения элементов орбит небольших частиц под влиянием длительного действия эффекта Пойнтинг—Робертсона, которое может дать нам представление о времени, когда произошло отделение, а следовательно, и о возрасте потока. Для решения первого вопроса необходимо произвести достаточно точные определение большого количества радиантов слабых метеоров потока, что при современных технических средствах можно сделать только при помощи телескопа, а также определение их гелиоцентрических скоростей с точностью, большей чем посредством радара. Решение второго вопроса связано с количеством слабых метеоров в потоке, что можно решить только при помощи соответственно приспособленного метода телескопического или радарного наблюдения; из этих двух способов телескопические наблюдения до сих пор позволяют исследовать мелчайшие частицы и имеют, следовательно, большие перспективы на успех.

При наблюдениях метеоров посредством телескопа или радара фактором помех является фон спорадических метеоров, который гораздо труднее исключить, чем при визуальных и фотографических наблюдениях. Главной задачей нашей работы являлось определить свойства этого фона, найти наиболее подходящий способ для исключения его влияния при наблюдениях метеорных потоков, и одновременно разработать другой независимый способ для статистического

определения активности потоков, к способу приведенному в другой статье настоящего сборника.

Необходимо было проверить правильность теоретических выводов, основанных на довольно сложных предпосылках, путем непосредственного наблюдения; поэтому в настоящей работе розработано наблюдений более 1000 телескопических метеоров, произведенных в 1946—1953 гг. в астрономической обсерватории Словацкой Академии Наук в Скальнате Плесо. Что касается статистики направлений, то этот ряд наблюдений является наиболее обширным из всех до сих пор опубликованных. На основании этих наблюдений мы смогли решить и некоторые дальнейшие вопросы, которые связаны не с образованием метеорных потоков, но с геометрическими и физиологическими условиями видимости метеоров при телескопических наблюдениях. Кроме того были произведены исследования по распределению орбит телескопических метеоров в пространстве, особенно их отношение к апексу и эклиптике.

Из работы вытекают следующие основные заключения:

1. Кажущееся распределение направлений телескопических метеоров тесно связано с положением наблюдаемой области в горизонтальной системе координат. Эта зависимость имеет значительно большее значение, чем все остальные факторы, проявляющиеся в статистике направлений, т. е. инструментальные и физиологические влияния, влияние формы, тяготения и движения Земли, а также расположение метеорных орбит в солнечной системе.

2. На основании геометрических соображений удалось вывести стандартное распределение направлений, которое очень точно совпадает с результатами наблюдений. Поправки на искривление атмосферы и зенитное притяжение были выражены формулами и включены в окончательные результаты.

3. Было произведено сравнение формул Гофмейстера и Прентиса для вычисления зенитной частоты метеорных потоков с формулами, которые косвенно вытекают из нашей теории. Было установлено, что при телескопических наблюдениях надо принимать меньшие отклонения от простого закона $F \sim \cos z$, чем обычно указывают.

4. Непосредственные наблюдения показывают, что видимость телескопических метеоров практически не зависит от угла, под которым метеоры попадают в атмосферу Земли.

5. Было доказано, что при применении нормального телескопа, подходящего для телескопических наблюдений метеоров (диаметр 10 см, увеличение в 25 раз, поле зрения 3,6°) селекция ограниченного поля зрения выравнивает селекцию разных угловых скоростей, так что при статистике направлений не надо принимать во внимание инструментальные и физиологические влияния.

6. Даже при увеличении в 25 раз влияние увеличения угловой скорости не настолько значительно, чтобы дать возможность наблюдать метеоры только вблизи радианта, как предполагают некоторые авторы.

7. Определение стандартного распределения направлений обеспечило возможность произвести более подробные исследования анизотропии направлений движения метеоров вблизи Земли. Кажущееся движение метеоров от апекса к антиапексу, вызываемое движением Земли вокруг Солнца, ясно проявляется при наблюдениях. Кроме того, установлена также концентрация метеорных орбит к плоскости эклиптики, которая вместе с большим количеством прямых движений по сравнению с обратными показывает, что орбиты части телескопических метеоров похожи на орбиты некоторых малых планет или эклиптикальных потоков.

8. Движение метеоров по направлению к Солнцу, установленное Эпиком и Бахаревым, удалось объяснить селекцией, как только кажущееся.

9. Для телескопических наблюдений метеорных потоков был выработан специальный метод, который дает возможность установить наличие и число слабых метеоров в разных потоках, в том числе и при очень рассеянных радиантах. Метод разработан таким образом, что одновременно дает возможность определять и размеры и вид области радиации. При помощи подробных таблиц, основанных на принципах теории вероятности, можно надежно определить, является ли известный радиант телескопически активным или нет.

ĽUBOR KRESÁK

ROZDELENIE SMEROV TELESKOPICKÝCH METEOROV

V poslednom čase venuje sa stále väčšia pozornosť najmenším pevným čiastočkám medziplanetárnej hmoty a ich postaveniu v slnečnej sústave. Presné fotografické merania polôh a rýchlostí meteorov, ktoré za dnešného stavu nám jediné môžu podať bližšie informácie o heliocentrických dráhach týchto telies, prakticky sa obmedzujú na čiastočky o hmotách rádu 10^{-2} až 10 gramov. Hmoty pod 10^{-2} gramov pripadajú na slabé vizuálne a teleskopické meteory, ktoré tvoria prirodzený prechod k neviditeľným prachovým čiastočkám. Najnovšie výskumy naznačujú, že na neviditeľný prach pripadá oveľa väčší prínos hmoty Zeme ako na viditeľné meteory. Pritom naše vedomosti o dráhach týchto telies sú veľmi neisté a analógia s jasnými meteormi nezdá sa byť nijako opodstatnená.

Medzi najnaliehavejšie problémy meteorickej astronómie patrí otázka, či, v akom počte a v akom usporiadaní sú neviditeľné prachové čiastočky obsažené v meteorických rojoch rôznych typov. Z hľadiska vzniku a vývoja meteorických rojov zaslúžia si osobitnú pozornosť dve otázky, ktorých rozriešenie možno hľadať už v oblasti teleskopických meteorov. Po prvé je to závislosť rozptylu dráh od veľkosti meteorov, ktorá nám môže podať určitý obraz o rozdelení impulzu medzi rojové meteory pri ich odlúčení od materskej kométy (prípadne aj pri inom procese vzniku) a tým i o podmienkach vytvorenia roja. Po druhé je to zistenie systematického posunutia dráh menších častíc pod vplyvom dlhého pôsobenia Poynting—Robertsonovho efektu, ktoré nám môže podať informáciu o čase, kedy k odlúčeniu došlo, a teda aj o veku roja. Riešenie prvej otázky predpokladá určenie veľkého počtu presných radiantov slabých rojových meteorov, ktoré je pri dnešných technických prostriedkoch možné iba teleskopicky a určenie ich heliocentrických rýchlostí s väčšou presnosťou ako dávajú radarové merania. Riešenie druhej otázky súvisí s početnosťou slabých meteorov v roji, o ktorej možno rozhodnúť iba vhodne prispôsobenou metódou teleskopického alebo radarového pozorovania; z obidvoch metód však teleskopické pozorovanie má nateraz väčší dosah a tým aj väčšiu nádej na úspech.

Pri pozorovaniach ďalekohľadom alebo radarom vystupuje ako rušivý faktor pozadie sporadických meteorov, ktoré sa dá oveľa ľažšie eliminovať ako pri vizuálnych a fotografických pozorovaniach. Hlavnou úlohou našej práce bolo určiť vlastnosti tohto pozadia, nájsť najvhodnejší spôsob na potlačenie jeho vplyvu pri pozorovaniach meteorických rojov a vytvoriť súčasne druhú, celkom nezávislú metódu doplňujúcu štatistické zisťovanie činnosti rojov, o ktorom sa zmieňujeme na inom mieste tohto zborníka.

Platnosť teoretických vývodov, založených na určitých predpokladoch, bolo treba na mnohých miestach verifikovať priamym pozorovaním; preto práca obsahuje aj redukcie pozorovaní vyše 1000 teleskopických meteorov, vykonaných v rokoch 1946—1953 na Astronomickom observatóriu SAV na Skalnatom Plese. Čo sa týka štatistiky smerov, tento pozorovací rad je zo všetkých doteraz publikovaných radov najobsiahlejší. Preto sa na ňom dali riešiť aj niektoré ďalšie problémy, ktoré nesúvisia s vývojom meteorických rojov, ale s geometrickými a fyziologickými podmienkami viditeľnosti meteorov pri teleskopickom pozoro-

aní. Okrem toho bolo skúmané rozdelenie dráh teleskopických meteorov v priestore, najmä pokiaľ sa prejavuje vo vzťahu k apexu a k ekliptike.

Z práce vyplynuli tieto hlavné závery:

1. Zdanlivé rozdelenie smerov teleskopických meteorov úzko súvisí s polohou pozorovanej oblasti v horizontálnom súradnicovom systéme. Táto závislosť ďaleko prevyšuje všetky ostatné faktory, ktoré sa prejavujú v štatistike smerov, t. j. prístrojové a fyziologické vplyvy, vplyv tvaru, príťažlivosti a pohybu Zeme, alebo usporiadanie meteorických dráh v slnečnej sústave.

2. Z geometrických úvah podarilo sa odvodiť štandardné rozdelenie smerov, ktoré veľmi dobre súhlasí s pozorovaním. Opravy na zakrivenie atmosféry a zenitovú atrakciu boli vyjadrené vzorcami a zahrnuté do definitívnych výpočtov.

3. Hoffmeistrov a Prenticov vzorec pre výpočet zenitovej frekvencie meteorických rojov boli porovnané s tými, ktoré nepriamo vyplývajú z našej teórie. Ukázalo sa, že pre teleskopické pozorovania treba prijať menšie odchýlky od jednoduchého kosínového zákona, ako sa bežne udávajú pre vizuálne pozorovania.

4. Z pozorovaní možno odvodiť, že viditeľnosť teleskopických meteorov je prakticky nezávislá od uhla, pod ktorým vnikajú do zemskej atmosféry.

5. Bolo dokázané, že pre normálny ďalekohľad, vhodný pre teleskopické pozorovania meteorov (priemer 10 cm, zväčšenie 25-násobné, zorné pole 3,6°) výberový efekt ohraničeného zorného poľa približne vyrovnáva výberový efekt rôznych uhlových rýchlostí, takže prístrojové a fyziologické vplyvy pri štatistike smerov netreba brať do úvahy.

6. Ani pri 25-násobnom zväčšení nie je vplyv zväčšenej uhlovej rýchlosti taký, aby dovolil pozorovať meteory iba v blízkom okolí radiantu, ako niektorí autori predpokladajú.

7. Odvodenie štandardného rozdelenia smerov umožnilo bližšie preskúmať anizotropiu smerov pohybu meteorov v blízkosti Zeme. Zdanlivé prúdenie meteorov od apexu k antapexu, vyvolané pohybom Zeme okolo Slnka, sa na pozorovaniach zreteľne prejavuje. Okrem toho sa ukázala určitá koncentrácia meteorických dráh k rovine ekliptiky, ktorá spolu s prevahou priamych pohybov nad retrográdnymi poukazuje na to, že dráhy časti teleskopických meteorov pripomínajú dráhy malých planét a ekliptikálnych rojov.

8. Prúdenie teleskopických meteorov smerom k Slnku, ktoré zistili Oepik a Bacharev, podarilo sa vysvetliť výberovým efektom ako zdanlivé.

9. Pre teleskopické pozorovania meteorických rojov bola odvodená špeciálna metóda, ktorá dovoľuje zistiť prítomnosť a početnosť slabých meteorov v rôznych rojoch, a to aj pri veľmi difúznych radiantoch. Metóda je upravená tak, aby sa súčasne dali určiť tiež rozmery a tvar radiačnej oblasti. Pomocou podrobných tabuliek, založených na zákonoch počtu pravdepodobnosti, dá sa spoľahlivo zistiť, či je určitý radiant teleskopicky aktívny alebo nie.